

The TRPM2 ion channel is required for sensitivity to warmth

Chun-Hsiang Tan^{1,2} & Peter A. McNaughton¹

Thermally activated ion channels are known to detect the entire thermal range from extreme heat (TRPV2), painful heat (TRPV1, TRPM3 and ANO1), non-painful warmth (TRPV3 and TRPV4) and non-painful coolness (TRPM8) through to painful cold (TRPA1)^{1–7}. Genetic deletion of each of these ion channels, however, has only modest effects on thermal behaviour in mice^{6–12}, with the exception of TRPM8, the deletion of which has marked effects on the perception of moderate coolness in the range 10–25 °C¹³. The molecular mechanism responsible for detecting non-painful warmth, in particular, is unresolved. Here we used calcium imaging to identify a population of thermally sensitive somatosensory neurons which do not express any of the known thermally activated TRP channels. We then used a combination of calcium imaging, electrophysiology and RNA sequencing to show that the ion channel generating heat sensitivity in these neurons is TRPM2. Autonomic neurons, usually thought of as exclusively motor, also express TRPM2 and respond directly to heat. Mice in which TRPM2 had been genetically deleted showed a striking deficit in their sensation of non-noxious warm temperatures, consistent with the idea that TRPM2 initiates a ‘warm’ signal which drives cool-seeking behaviour.

Previous studies have described novel heat-sensitive neurons not activated by agonists for any of the known heat-sensitive ion channels^{5,14–16}. We identified these neurons in cultures from dorsal root ganglia (DRG) by using calcium imaging and selective agonists for known thermo-TRP ion channels. We found that around 10% of neurons responded to heat, but were not activated by any of the agonists for known TRP channels (Fig. 1a–c and Supplementary Video 1). Changing the order of application of agonists or using a lower starting temperature had little effect on this proportion (Extended Data Figs 1 and 2). Novel heat-sensitive neurons were found to be activated over a wide range of temperatures, with a subset activated in the range of warm temperatures between 34 °C and 42 °C, suggesting a possible role in warmth sensation, and a second group activated only at higher temperatures (Fig. 1d, e). Novel heat-sensitive neurons were significantly larger than either TRPV1-expressing or TRPM3-expressing neurons (Extended Data Fig. 3). We investigated the possibility that the novel heat-sensitivity may be co-expressed with TRPV1 and TRPM3 by blocking these channels with antagonists before applying heat; the higher proportion of neurons responding (46% in Extended Data Fig. 4a, compared to <10% expressing only the novel heat-sensitive mechanism, see Fig. 1 and Extended Data Figs 1, 2 and 4b) shows that there is significant co-expression of the novel heat-sensitive mechanism with TRPV1 and TRPM3. The phenotype of neurons expressing the novel heat-sensitive mechanism was investigated by identifying novel heat-sensitive neurons in the presence of TRP channel blockers (Extended Data Fig. 5a, red) and then exposing them to IB4, which marks a non-peptidergic neuronal population (Extended Data Fig. 5b, green). These results show that the novel heat-sensitive mechanism is predominantly expressed in IB4⁺ neurons (74% IB4⁺).

We next sought to identify a source of neurons which expresses a less-complex set of heat-sensitive ion channels than are present in DRG neurons. In isolated sympathetic neurons from the superior cervical ganglion (SCG) we found that no neuron showed an increase in intracellular calcium concentration ($[Ca^{2+}]_i$) in response to agonists of known thermo-TRP channels, but that 58% showed a significant response to heat (Fig. 2a and Extended Data Fig. 6). Similar results were obtained in parasympathetic neurons isolated from the pterygo-palatine ganglion (PPG), in which 49% of neurons showed novel heat sensitivity (not shown). Autonomic neurons therefore express the novel heat-activated ion channel in isolation, which offers an advantageous preparation for determining its properties.

We found that the heat-activated calcium increase in autonomic neurons was due to an influx of Ca^{2+} from the external solution, and that it was reduced but not abolished by removal of external Na^+ (Extended Data Fig. 6c). The TRPV channel family activator 2-APB¹⁷ suppressed the heat-activated Ca^{2+} influx, and the TRPV blocker ruthenium red² had no effect (Extended Data Fig. 6d, e), making it unlikely that the novel heat-activated mechanism is a TRPV family member. The Ca^{2+} influx was unaffected by the voltage-dependent Na^+ channel blocker tetrodotoxin (TTX) at a high enough concentration to block the TTX-insensitive Na^+ channels $Nav1.8$ and $Nav1.9$ (Extended Data Fig. 6f). L-type Ca^{2+} channel blockers prevented firing of action potentials during simultaneous recordings of membrane voltage and intracellular calcium imaging, but did not completely block the heat-activated Ca^{2+} influx (Fig. 2b; see also Extended Data Fig. 6g). Together these observations show that the heat-sensitive ion channel is permeable both to Ca^{2+} and to Na^+ , and that when the channel is opened by heat, the resulting depolarization activates L-type calcium channels and thus augments the calcium influx. The fact that membrane current through the novel heat-activated ion channel is carried by Na^+ and Ca^{2+} makes it unlikely that the channel is ANO1, which is permeable to chloride ions⁶.

We next investigated the voltage- and time-dependent behaviour of the novel heat-activated ion channel, isolated by suppressing voltage-dependent calcium, sodium and potassium currents¹. The current-voltage relation was approximately linear, with a reversal potential close to zero (Fig. 2c), and the channel showed no time-dependent gating by membrane voltage (Extended Data Fig. 7). Interestingly, activation of the channel by mild warmth was strongly potentiated by hydrogen peroxide, both in autonomic neurons (Fig. 2d) and in DRG neurons (Extended Data Fig. 4c, d).

To identify the ion channel responsible for the novel heat sensitivity we carried out an analysis of mRNA expression by the use of RNA sequencing (RNA-seq). We investigated two cell lines, MAH cells¹⁸ and PC12 cells, both derived from rat adrenal cells, which share many properties with sympathetic neurons. Like primary autonomic neurons, no cell in either line responded to agonists of any of the conventional thermo-TRP channels, but a significant fraction of cells responded to heat with thermal thresholds similar to those in somatosensory neurons

¹Wolfson Centre for Age-Related Diseases, King's College London, Guy's Campus, London Bridge, London SE1 1UL, UK. ²Department of Neurology, Kaohsiung Medical University Hospital, Kaohsiung Medical University, Kaohsiung, Taiwan.

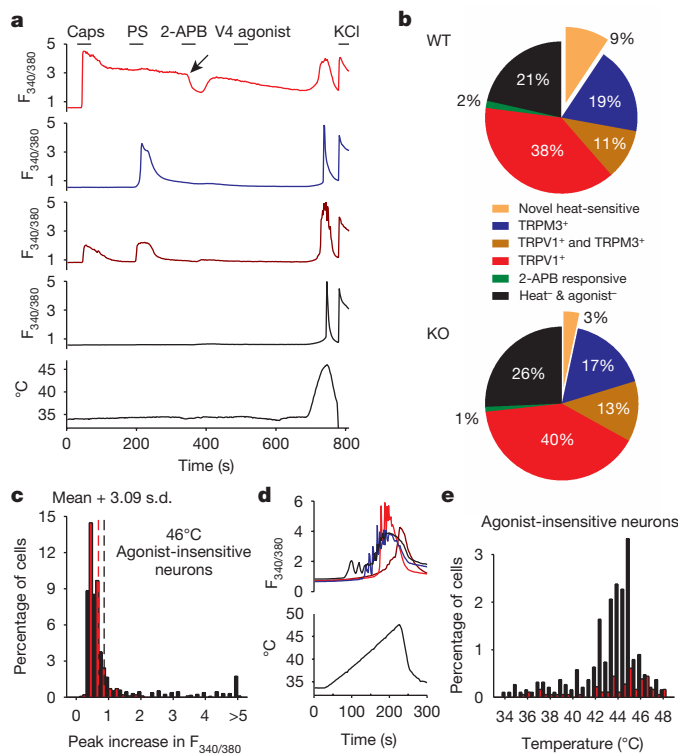


Figure 1 | Around 10% of somatosensory neurons demonstrate a novel heat-sensitive response. **a**, Examples of increases of $[Ca^{2+}]_i$ measured with fura-2 ($F_{340/380}$ ratio, ordinate) in response to known TRP channel agonists and to heat. From top: TRPV1-expressing neuron responding to capsaicin (caps, red); TRPM3-expressing neuron responding to pregenolone sulfate (PS, blue); TRPV1- and TRPM3-co-expressing neuron (brown); neuron unresponsive to TRP channel agonists but showing a response to heat (bottom trace). See Supplementary Information Video 1. **b**, Percentages of neurons expressing TRPV1, TRPM3 and the novel heat-sensitive mechanism in DRG neurons from wild-type (WT) (top) and *Trpm2*^{-/-} knockout (KO) mice (bottom). Green: neurons responding to 2-APB but not to other agonists. **c**, Histogram of maximal $F_{340/380}$ ratio increase in neurons insensitive to TRP agonists. Black, wild-type neurons; red, *Trpm2*^{-/-} neurons. Vertical dashed lines: thresholds discriminating between heat-sensitive and insensitive neurons (see Extended Data Fig. 1). **d**, Thermal thresholds of novel heat-sensitive DRG neurons. Increases of $F_{340/380}$ ratio in response to slowly rising heat ramp (bottom). **e**, Temperature thresholds of novel heat-sensitive neurons from wild-type (black) and *Trpm2*^{-/-} mice (red). Proportion in range 34–42 °C reduced from 4.4% in wild type to 0.9% in *Trpm2*^{-/-} ($P \leq 0.0001$; Fisher's exact test), and in range 42–48 °C from 15% in wild type (290/1,890) to 3% in *Trpm2*^{-/-} (55/1,800) ($P \leq 0.0001$; Fisher's exact test). Cell numbers and replicates for **a–c** were 1,324 DRG neurons from one wild-type mouse on 4 coverslips and 981 DRG neurons from one *Trpm2*^{-/-} mouse on 4 coverslips were imaged. Similar results obtained using 52 additional coverslips from 9 additional wild-type mice and 10 coverslips from 3 additional *Trpm2*^{-/-} mice; some of these results are shown in Extended Data Figs 1, 2 and 4. Cell numbers and replicates for **d** and **e** were 1,890 DRG neurons from one wild-type mouse on 8 coverslips and 1,800 DRG neurons from one *Trpm2*^{-/-} mouse on 8 coverslips were imaged. Similar results obtained using 10 coverslips from one additional wild-type mouse.

(Extended Data Fig. 8). We also found that the fraction of heat-sensitive neurons in both lines was reduced by differentiation to a neuronal-like phenotype (Extended Data Fig. 8, red bars).

The properties of mixed Na^+/Ca^{2+} permeability, a reversal potential near 0 mV and absence of time-dependent gating by membrane potential (see earlier) are consistent with a member of the large TRP and CNG ion channel families. RNA-seq analysis of the MAH cell line showed that detectable mRNA was present only for the seven TRP channels shown in Table 1, out of all TRP and CNG channels. TRPC3, TRPV2, TRPM4 and TRPM7 are unlikely candidates for the warmth-sensitive

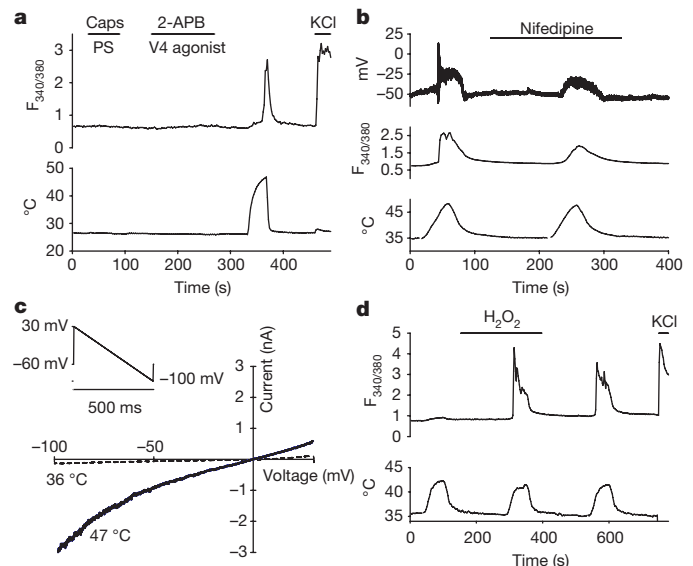


Figure 2 | Properties of the novel heat-sensitive ion channel in autonomic neurons. **a**, Sympathetic neurons from superior cervical ganglion (SCG) respond to heat but not to TRP channel agonists. **b**, The L-type Ca^{2+} channel blocker nifedipine (10 μ M) blocks spiking but not steady depolarization in response to heat in a patch-clamped PPG neuron (top), and reduces, but does not eliminate the Ca^{2+} increase (middle). Simultaneous recording of membrane potential and $[Ca^{2+}]_i$ ($F_{340/380}$ ratio) in current-clamped PPG neuron. **c**, Current–voltage relations at 36 °C and 47 °C of voltage-clamped PPG neuron in response to voltage ramp shown in the top left. Similar I/V relation observed with inverse voltage ramp starting from –100 mV (Extended Data Fig. 7). See Methods for details. **d**, H_2O_2 (400 μ M) potentiates Ca^{2+} increase in response to a mild temperature stimulus (42 °C) in SCG neurons. Note potentiation is long-lasting after H_2O_2 is removed. Similar results obtained in PPG neurons. Percentage of neurons ($n = 456$) responding to heat, determined as in Extended Data Fig. 1b, was 5% before, 59% during and 54% post- H_2O_2 , respectively. Cell numbers and replicates for **a** were 166 SCG neurons from 3 wild-type mice on 3 coverslips imaged for this experiment. Similar results obtained with SCG neurons using 15 additional coverslips from 9 additional mice and with PPG neurons using 14 coverslips from 9 additional mice. Cell numbers and replicates for **b** were 2 PPG neurons on 2 coverslips simultaneously patch-clamped and imaged and these showed a similar response. Cell numbers and replicates for **c** were 3 PPG neurons on 3 coverslips simultaneously patch-clamped and imaged and these showed a similar enhancement with H_2O_2 ; 731 PPG neurons (not shown) from three wild-type mice on 3 coverslips were imaged and showed a similar enhancement to the SCG neurons. Similar results obtained with SCG neurons using 9 coverslips from 5 additional mice and with PPG neurons using 3 coverslips from 3 additional mice.

channel as all have nonlinear current–voltage (I/V) relations¹⁹, whereas the warmth-sensitive ion channel is linear (Fig. 2c). TRPC1 and TRPV2 are strongly upregulated by culture in differentiation medium (Table 1), which contrasts with the downregulation observed for the heat-sensitive ion channel (Extended Data Fig. 8a). TRPV2 is activated only by extreme heat²⁰ and TRPM4 is calcium-impermeable²¹, neither of which is consistent with the properties of the novel heat-sensitive ion channel (see above). *TRPC2* is a pseudogene in primates and seems unlikely to play an important role in behavioural warmth sensation, a fundamental property in all mammals. This leaves only TRPM2, which has a linear I/V relation (see Fig. 2c)²², is activated at temperatures above 35 °C²² and is expressed in DRG neurons^{23,24}, as the most probable candidate for the warmth-sensitive ion channel. Thermal activation of TRPM2 is enhanced by hydrogen peroxide²⁵ and the channel is blocked by the chemical 2-APB²⁶, both of which are characteristics shared by the novel heat-sensitive ion channel (Fig. 2d and Extended Data Figs 4c, d and 6d).

Table 1 | mRNA levels of TRP ion channel genes in MAH cells

Gene	FPKM in growth medium	FPKM in differentiation medium	Log ₂ fold change	<i>P</i> value	<i>q</i> value
<i>Trpc1</i>	1.779	4.700	1.401	<0.001	<0.001
<i>Trpc2</i>	6.804	4.995	-0.446	0.121	0.323
<i>Trpc3</i>	5.641	1.309	-5.729	<0.001	<0.001
<i>Trpv2</i>	0.035	4.003	6.840	<0.001	<0.001
<i>Trpm2</i>	1.017	0.970	-0.069	0.800	0.922
<i>Trpm4</i>	0.277	0.400	0.532	0.112	0.310
<i>Trpm7</i>	18.108	15.428	-0.231	0.196	0.428

All genes within the TRP channel family and the six cyclic nucleotide-regulated channels (*Cnga1*, *Cnga2*, *Cnga3*, *Cnga4*, *Cngb1*, and *Cngb3*) were examined. The seven genes listed are the ones whose mRNA levels are detectable in MAH cells in either condition. FPKM, fragments per kilobase of transcript per million mapped reads. The *P* values represent significance of change of expression using one-way ANOVA; *q* values are post-hoc corrected for multiple testing using the false discovery rate (FDR) method. Two biological replicates in each condition were deep-sequenced. Growth medium contained dexamethasone (5 μM), differentiation medium contained the growth factors bFGF (10 ng ml⁻¹), CNTF (10 ng ml⁻¹) and NGF (50 ng ml⁻¹).

We confirmed the identity of the novel heat-sensitive ion channel using calcium imaging experiments on neurons from *Trpm2*^{-/-} mice^{27,28}. The proportions of DRG neurons responding to TRP channel agonists were similar to those in wild-type neurons (Fig. 1b and Extended Data Figs 1c and 2c), but the proportion of novel heat-sensitive neurons was significantly reduced, from ~10% to around 3% (Fig. 1c, red bars; *P* ≤ 0.0001, Fisher's exact test, see also Extended Data Figs 1, 2 and 4). Moreover, the mean amplitude of the increase in the fura-2 fluorescence ratio at 340 and 380 nm (an index of the increase in intracellular calcium) in *Trpm2*^{-/-} neurons not responding to TRP channel agonists was greatly reduced, from $F_{340/380} = 2.336 \pm 0.2060$ in wild type, to 0.6202 ± 0.2435 in *Trpm2*^{-/-} (Fig. 1c; *P* ≤ 0.0001, two-tailed unpaired *t*-test). Notably, the sensitivity of the heat response to hydrogen peroxide was abolished by deletion of *Trpm2* (Extended Data Fig. 4c, d). In experiments on the thermal thresholds of novel heat-sensitive neurons (Fig. 1d, e), deletion of *Trpm2* abolished almost all thermal sensitivity in the range 34–42 °C (reduced from 4.4% in wild type to 0.9% in *Trpm2*^{-/-}, *P* ≤ 0.0001; Fisher's exact test), though some neurons still responded to temperatures in the noxious thermal range (reduced from 15% in wild type to 3.1% in *Trpm2*^{-/-}, *P* ≤ 0.0001; Fisher's exact test). We also considered the possibility that TRPM2 may contribute to the heat response in DRG neurons in which it is co-expressed with TRPV1 and/or TRPM3. Deletion of *Trpm2* was found not to affect the maximum amplitude of the response to heat in TRPV1-expressing neurons, but it did reduce the response of TRPM3-expressing neurons (Extended Data Fig. 9), suggesting that co-activation of TRPM2 and TRPM3 is important in determining the heat responses of these neurons. Finally, in SCG neurons from *Trpm2*^{-/-} mice, both the numbers and response amplitudes of heat-sensitive neurons were greatly reduced (Extended Data Fig. 6b).

Expression of mRNA that encodes TRPM2 was demonstrated in heat-sensitive DRG neurons using *in situ* hybridization. *Trpm2* mRNA was surprisingly abundant in neurons, being expressed in 89% of DRG neurons, but was expressed in, at most, a very small minority of glial cells (Extended Data Fig. 10). In prior tests for heat sensitivity in the same neurons, 42% of neurons positive for *Trpm2* mRNA had responded when TRPV1 and TRPM3 were blocked. The reason why not all neurons positive for *Trpm2* mRNA respond to heat is not clear, but could be due to a low conversion of mRNA into TRPM2 protein or to low trafficking to the membrane in around half of DRG neurons. However, many fewer neurons responded to heat in the population not expressing mRNA for *Trpm2* (13%, see Extended Data Fig. 10), which is consistent with the small number of heat-sensitive neurons still seen in DRG cultures from *Trpm2*^{-/-} mice (see for example, Fig. 1b).

Finally, we investigated whether genetic deletion of *Trpm2* has an impact on thermal preference in mice. The most striking behavioural difference was that wild-type mice avoided the non-noxious warm temperature of 38 °C, whereas *Trpm2*^{-/-} mice showed little preference (Fig. 3c, e and Supplementary Video 2). The difference became much less noticeable at 43 °C, when noxious-heat avoidance mechanisms

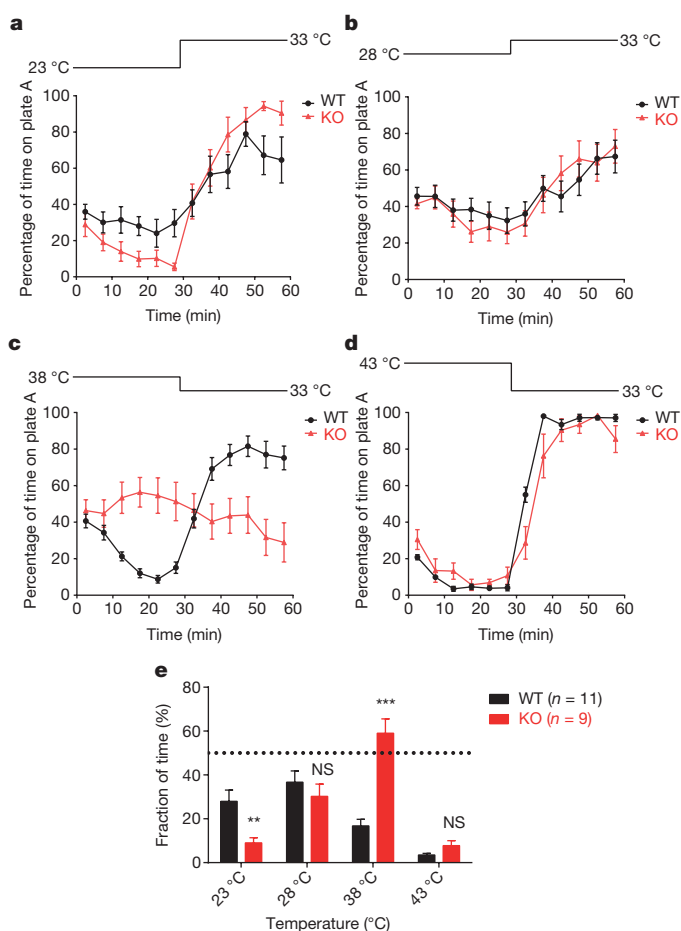


Figure 3 | Deletion of TRPM2 shifts adult male mouse thermal preference towards warmer temperatures. a–d, Two-plate thermal preference test. One plate is at 33 °C at the start of the experiment, the other ('plate A') is at a variable temperature as shown above each graph. Temperature reversed at *t* = 30 min to account for any possible bias caused by external cues. Points show mean behavioural preference averaged over 5 min intervals (error bars represent the mean ± s.e.m., *n* = 11 for wild type and 9 for *Trpm2*^{-/-}). Mice were wild-type or *Trpm2*^{-/-} (KO) male littermates, aged 12–16 weeks of age. No difference was observed between the thermal behaviour of wild-type and heterozygous *Trpm2*^{+/-} mice (not shown, *n* = 4). e, Mean thermal preference averaged from the data between *t* = 15–30 min and *t* = 45–60 min shown in a–d. Error bars represent the mean ± s.e.m. ***P* < 0.01; ****P* < 0.001; NS, *P* > 0.05; unpaired *t*-test. Similar results were obtained with experiments using non-littermates in which 12 wild-type male mice from Charles River were compared with 7 *Trpm2*^{-/-} male mice from homozygote breeding pairs.

driven by TRPV1, TRPM3 and ANO1 become important^{3–9}. Wild-type mice also showed a less strong aversion than *Trpm2*^{-/-} mice for the non-noxious cool temperature of 23 °C (Fig. 3a, e). Expression of TRPM2 therefore causes wild-type mice to prefer cooler temperatures over a range of temperatures extending from 23 °C to above 38 °C, though we note that the actual temperature at the sensory nerve ending will be higher than the plate temperature, particularly at the lower end of this range, because of the influence of body temperature.

The work presented here shows that TRPM2 accounts for a novel heat-sensitive mechanism in both somatosensory and autonomic neurons. The altered thermal preference in *Trpm2*^{-/-} mice supports the hypothesis that TRPM2 expressed in somatosensory neurons provides a non-noxious 'warm' signal which drives mice to seek cooler temperatures over a wide temperature range, from 23 °C to above 38 °C. Other studies have shown that TRPM8 provides a 'cool' signal which drives warmth-seeking behaviour over the range 10–25 °C¹³, whereas activation of TRPV1, TRPM3 and ANO1 provide a high-temperature noxious-heat-avoidance signal^{3–9}.

Online Content Methods, along with any additional Extended Data display items and Source Data, are available in the online version of the paper; references unique to these sections appear only in the online paper.

Received 5 June 2015; accepted 1 July 2016.

Published online 17 August 2016.

- Cesare, P. & McNaughton, P. A novel heat-activated current in nociceptive neurons and its sensitization by bradykinin. *Proc. Natl Acad. Sci. USA* **93**, 15435–15439 (1996).
- Caterina, M. J. *et al.* The capsaicin receptor: a heat-activated ion channel in the pain pathway. *Nature* **389**, 816–824 (1997).
- Jordt, S. E., McKemy, D. D. & Julius, D. Lessons from peppers and peppermint: the molecular logic of thermosensation. *Curr. Opin. Neurobiol.* **13**, 487–492 (2003).
- Basbaum, A. I., Bautista, D. M., Scherrer, G. & Julius, D. Cellular and molecular mechanisms of pain. *Cell* **139**, 267–284 (2009).
- Vriens, J. *et al.* TRPM3 is a nociceptor channel involved in the detection of noxious heat. *Neuron* **70**, 482–494 (2011).
- Cho, H. *et al.* The calcium-activated chloride channel anoctamin 1 acts as a heat sensor in nociceptive neurons. *Nature Neurosci.* **15**, 1015–1021 (2012).
- Vriens, J., Nilius, B. & Voets, T. Peripheral thermosensation in mammals. *Nature Rev. Neurosci.* **15**, 573–589 (2014).
- Caterina, M. J. *et al.* Impaired nociception and pain sensation in mice lacking the capsaicin receptor. *Science* **288**, 306–313 (2000).
- Davis, J. B. *et al.* Vanilloid receptor-1 is essential for inflammatory thermal hyperalgesia. *Nature* **405**, 183–187 (2000).
- Moqrich, A. *et al.* Impaired thermosensation in mice lacking TRPV3, a heat and camphor sensor in the skin. *Science* **307**, 1468–1472 (2005).
- Huang, S. M., Li, X., Yu, Y., Wang, J. & Caterina, M. J. TRPV3 and TRPV4 ion channels are not major contributors to mouse heat sensation. *Mol. Pain* **7**, 37 (2011).
- Miyamoto, T., Petrus, M. J., Dubin, A. E. & Patapoutian, A. TRPV3 regulates nitric oxide synthase-independent nitric oxide synthesis in the skin. *Nature Commun.* **2**, 369 (2011).
- Bautista, D. M. *et al.* The menthol receptor TRPM8 is the principal detector of environmental cold. *Nature* **448**, 204–208 (2007).
- Nagy, I. & Rang, H. Noxious heat activates all capsaicin-sensitive and also a sub-population of capsaicin-insensitive dorsal root ganglion neurons. *Neuroscience* **88**, 995–997 (1999).
- Woodbury, C. J. *et al.* Nociceptors lacking TRPV1 and TRPV2 have normal heat responses. *J. Neurosci.* **24**, 6410–6415 (2004).
- Lawson, J. J., McIlwrath, S. L., Woodbury, C. J., Davis, B. M. & Koerber, H. R. TRPV1 unlike TRPV2 is restricted to a subset of mechanically insensitive cutaneous nociceptors responding to heat. *J. Pain* **9**, 298–308 (2008).
- Hu, H. Z. *et al.* 2-aminoethoxydiphenyl borate is a common activator of TRPV1, TRPV2, and TRPV3. *J. Biol. Chem.* **279**, 35741–35748 (2004).
- Birren, S. J. & Anderson, D. J. A v-myc-immortalized sympathoadrenal progenitor cell line in which neuronal differentiation is initiated by FGF but not NGF. *Neuron* **4**, 189–201 (1990).
- Wu, L.-J., Sweet, T.-B. & Clapham, D. E. International Union of Basic and Clinical Pharmacology. LXXVI. Current progress in the mammalian TRP ion channel family. *Pharmacol. Rev.* **62**, 381–404 (2010).
- Caterina, M. J., Rosen, T. A., Tominaga, M., Brake, A. J. & Julius, D. A capsaicin-receptor homologue with a high threshold for noxious heat. *Nature* **398**, 436–441 (1999).
- Vennekens, R. & Nilius, B. Insights into TRPM4 function, regulation and physiological role. *Handb. Exp. Pharmacol.* **179**, 269–285 (2007).
- Togashi, K. *et al.* TRPM2 activation by cyclic ADP-ribose at body temperature is involved in insulin secretion. *EMBO J.* **25**, 1804–1815 (2006).
- Naziroglu, M., Ozgul, C., Celik, O., Cig, B. & Sozibir, E. Aminoethoxydiphenyl borate and flufenamic acid inhibit Ca²⁺ influx through TRPM2 channels in rat dorsal root ganglion neurons activated by ADP-ribose and rotenone. *J. Membr. Biol.* **241**, 69–75 (2011).
- Usoskin, D. *et al.* Unbiased classification of sensory neuron types by large-scale single-cell RNA sequencing. *Nature Neurosci.* **18**, 145–153 (2015).
- Hara, Y. *et al.* LTRPC2 Ca²⁺-permeable channel activated by changes in redox status confers susceptibility to cell death. *Mol. Cell* **9**, 163–173 (2002).
- Togashi, K., Inada, H. & Tominaga, M. Inhibition of the transient receptor potential cation channel TRPM2 by 2-aminoethoxydiphenyl borate (2-APB). *Br. J. Pharmacol.* **153**, 1324–1330 (2008).
- Yamamoto, S. *et al.* TRPM2-mediated Ca²⁺ influx induces chemokine production in monocytes that aggravates inflammatory neutrophil infiltration. *Nature Med.* **14**, 738–747 (2008).
- Uchida, K. *et al.* Lack of TRPM2 impaired insulin secretion and glucose metabolisms in mice. *Diabetes* **60**, 119–126 (2011).

Supplementary Information is available in the online version of the paper.

Acknowledgements We thank A. Tolkovsky for help and advice, R.-L. Yu for assistance with experiments, Y. Mori for *Trpm2*^{-/-} mice and for the cDNA for mouse TRPM2, S. Birren for MAH cells, J. Wood for loan of the thermal-preference test apparatus, S. Skerratt for PF-4674114, and E. Smith, J. Btesh, D. Andersson, and T. Bujs for their comments on the manuscript. Initial experiments were performed in the Department of Pharmacology, University of Cambridge. Supported by a grant from the BBSRC (UK) to P.A.McN. and a Raymond & Beverley Sackler studentship to C.-H.T.

Author Contributions C.-H.T. designed and performed experiments, analysed data and wrote the paper. P.A.M. designed experiments, analysed data, supervised the work and wrote the paper.

Author Information Reprints and permissions information is available at www.nature.com/reprints. The authors declare no competing financial interests. Readers are welcome to comment on the online version of the paper. Correspondence and requests for materials should be addressed to P.A.M. (peter.mcnaughton@kcl.ac.uk).

Reviewer Information *Nature* thanks M. Caterina, Y. Mori and the other anonymous reviewer(s) for their contribution to the peer review of this work.

METHODS

Animals. All *in vitro* experiments used C57BL/6 mice younger than 5 weeks old, except for adult DRG temperature threshold experiments (for example, Fig. 1c, d), in which 3-month-old adult mice were used (these mice were from the same group as was used for two-plate thermal preference tests experiments, see Fig. 3). *Trpm2*^{-/-} mice were gifts from Y. Mori, and were generated as reported previously^{27,28}. Mice were maintained on a 12 h day/12 h night cycle. All mice used in two-plate thermal preference tests had been backcrossed onto the parental C57Bl6/6J strain for 7 generations, and wild-type and *Trpm2*^{-/-} mice were littermates from breeding pairs of *Trpm2*^{+/-} heterozygote mice.

Primary neuron cultures. PPG, SCG and paravertebral chain ganglia were extracted from 3 or more mice and DRG from a single mouse. Ganglia were incubated in papain (2 mg ml⁻¹ in Ca²⁺-free and Mg²⁺-free HBSS) for 30 min at 30 °C, followed by incubation in collagenase (2.5 mg ml⁻¹ in Ca²⁺-free and Mg²⁺-free HBSS) for 30 min at 37 °C. Ganglia were re-suspended and mechanically dissociated in Neurobasal-A/B27 growing medium, which was prepared with Neurobasal-A Medium supplemented with 0.25% (v/v) L-glutamine 200 mM (Invitrogen), 2% (v/v) B-27 supplement (Invitrogen), 1% (v/v) penicillin-streptomycin (Invitrogen), and nerve growth factor (NGF) (Sigma-Aldrich) at 50 ng ml⁻¹. Dissociated neurons were centrifuged and plated onto coverslips pre-coated with poly-L-lysine (10 μg ml⁻¹) and laminin (40 μg ml⁻¹). Neurons were kept in a 37 °C incubator with a 95% air / 5% CO₂ atmosphere for at least 3 h before use, and all neurons were used within 24 h.

PC12 cell cultures. The growth medium used for PC12 cell culture was RPMI-1640 (Sigma-Aldrich), supplemented with: 1% (v/v) penicillin-streptomycin (Invitrogen), 1% (v/v) L-glutamine 200 mM (Invitrogen), 10% (v/v) horse serum (Invitrogen) and 5% (v/v) fetal bovine serum (FBS, Invitrogen). The differentiation medium for PC12 cells was RPMI-1640 supplemented with: 1% (v/v) penicillin-streptomycin (Invitrogen), 1% (v/v) L-glutamine-200 mM (Invitrogen), 1% (v/v) horse serum (Invitrogen), and NGF (Sigma-Aldrich) with final concentration at 100 ng ml⁻¹. PC12 cells were incubated and maintained in a 37 °C incubator with a 95% air / 5% CO₂ atmosphere. Medium was changed every 2 days, and cells were split every 3–4 days when grown to 90% confluency. The PC12 cells were seeded for imaging on coverslips pre-coated with poly-L-lysine (1 mg ml⁻¹; Sigma-Aldrich) and collagen IV (1 mg ml⁻¹; Sigma-Aldrich). PC12 cell lines were not authenticated and were not tested for mycoplasma contamination.

MAH cell cultures. MAH cells were kind gifts from A. Tolkovsky and S. Birren¹⁸. The growth medium used for MAH cell culture was L-15 medium (Sigma-Aldrich) supplemented with: 1% (v/v) penicillin-streptomycin (Invitrogen), 1% (v/v) L-glutamine 200 mM (Invitrogen), 10% (v/v) fetal bovine serum (FBS, Invitrogen), 17% (v/v) NaHCO₃ (150 mM), and dexamethasone (Sigma-Aldrich) at 5 μM. The differentiation medium for MAH cells was the same as the growth medium except dexamethasone was replaced with a cocktail of neurotrophic factors: CNTF (10 ng ml⁻¹; Peprotech), bFGF (10 ng ml⁻¹; Peprotech), and NGF (50 ng ml⁻¹; Sigma-Aldrich). Medium was changed every 2 days and MAH cells were split every 4 days when grown to 90% confluency and incubated and maintained in a 37 °C incubator with a 95% air / 5% CO₂ atmosphere. MAH cells used for imaging were seeded on coverslips pre-coated with poly-L-lysine (1 mg ml⁻¹; Sigma-Aldrich) and laminin (40 μg ml⁻¹; BD Science). MAH cell lines were not authenticated and were not tested for mycoplasma contamination.

Extracellular solutions and perfusion system for electrophysiology. Unless otherwise specified, all experiments were carried out with extracellular solution containing 140 mM NaCl, 4 mM KCl, 1.8 mM CaCl₂, 1 mM MgCl₂, 10 mM HEPES and 5 mM glucose; pH was adjusted to 7.4 with NaOH and osmolarity was between 295–305 mOsm. Sodium-free extracellular solution is prepared with the formulation above except for replacing sodium chloride with equimolar choline chloride. Calcium-free extracellular solution is prepared with the formulation above except for removal of calcium chloride. An 8-line manifold gravity-driven system controlled by an automated solution changer with a common outlet was used to apply solution to the cells. The temperature in three lines was heated or cooled with a Peltier device regulated by a proportional gain feedback controller designed by V. Vellani (CV Scientific). The temperature in each experimental protocol was recorded by a miniature thermocouple immediately before the solution entered the bath or (in separate control experiments) at the cell location at the tip of the solution outlet. All compounds applied were prepared as stock solutions first and then diluted to the concentration needed before experiments. Capsaicin was dissolved in ethanol to make 5 mM stock solutions. Pregnenolone sulphate was dissolved in DMSO to make 500 mM stock solutions. 2-APB was dissolved in DMSO to make 500 mM stock solutions. The TRPV4 agonist, PF-4674114, was dissolved in DMSO to make 5 mM stock solutions. Nifedipine was dissolved in DMSO to make 100 mM stock solutions. TTX was dissolved in pH 4.8 citrate buffer to make 100 mM stock solutions. Verapamil,

ruthenium red, and H₂O₂ were dissolved in extracellular solution on the day of experiments.

Calcium imaging. Cells were loaded with 5 μM fura-2 AM (Invitrogen) with 0.02% (v/v) pluronic acid (Invitrogen) for 30 min. After loading, coverslips were put in an imaging chamber and transferred to a Nikon Eclipse Ti-E inverted microscope. Cells were continuously perfused with extracellular solution and were illuminated with a monochromator alternating between 340 and 380 nm (OptoScan; Cairn Research), controlled by WinFluor 3.2 software (J. Dempster, University of Strathclyde, UK). Emission was collected at 510 nm and the resulting pairs of images were acquired every two seconds with a 100 ms exposure time using an iXon 897 EM-CCD camera (Andor Technology, Belfast, UK). Image time series were converted to TIFF files and processed with ImageJ software. Images of the background fluorescence intensity were obtained for both wavelengths and subtracted from the respective image stack before calculating the F_{340/380} ratio images. A minority of neurons (<10%) exhibited an unstable F_{340/380} baseline in the absence of any applied stimulus, usually caused by poor dye loading but in some cases apparently due to low-frequency repetitive firing even in the absence of any treatment, and were removed from analysis. In experiments to identify neurons responding to known TRP channel agonists (Fig. 1a), we found that PS caused a very slow increase in F_{340/380} ratio in some neurons, clearly distinguishable from the rapid elevation in [Ca]_i seen in TRPM3-expressing DRG neurons. This slow response can probably be attributed to an off-target effect of PS as it was also seen in autonomic neurons which do not appear to express TRPM3 (Fig. 2). A positive response to all agonists was therefore defined from the rate of increase of [Ca]_i following agonist application, as an increase of F_{340/380} ratio, between two consecutive time points following application of agonist, which exceeds the mean + 3.09 s.d. (cumulative probability value of 99.9%) of all such differences in the absence of any agonist. A heat-sensitive neuron is defined as a neuron with a peak increase in F_{340/380} during a heat stimulus larger than the mean + 3.09 s.d. of the peak increase in F_{340/380} of the glial cells in the same experiment (see Extended Data Fig. 1b). The thermal threshold of a heat-responsive neuron (see Fig. 1d, e) was defined as the temperature when the increase in F_{340/380} ratio between two consecutive time points is larger than the mean + 3.09 s.d. of the increase in F_{340/380} of the glial cells between two consecutive time points in the same experiment. For MAH and PC12 cell cultures, where no glial cells were present, we used the value of mean + 3.09 s.d. obtained from glial cells in similar experiments on neuronal cultures.

Supplementary Information Video 1 shows an example series of calcium images.

Patch clamp recordings. The intracellular solution for concurrent calcium imaging and patch clamp (see Fig. 2b) contained 140 mM KCl, 1.6 mM MgCl₂, 2.5 mM MgATP, 0.5 mM NaGTP, 10 mM HEPES and 167 μM fura-2; pH was adjusted to 7.3 with KOH. The intracellular solution for current-voltage relationship determination, in which Ca²⁺ and K⁺ currents were blocked (see Fig. 2c), contained 130 mM CsCl, 2.5 mM MgATP, 0.5 mM NaGTP, 10 mM HEPES, 10 mM TEA, and 5 mM 4-AP; pH was adjusted to 7.3 with CsOH. The osmolarity of both of the intracellular solutions was between 295–305 mOsm. The extracellular solution for current-voltage relationship determination contained 125 mM NaCl, 2 mM CaCl₂, 10 mM HEPES and 5 mM glucose, 10 mM TEA, 5 mM 4-AP, 2 μM tetrodotoxin, and 100 μM CdCl₂.

All patch clamp experiments were carried out with an Axopatch 200B patch-clamp amplifier (Axon Instrument, USA). Patch pipettes (Blaubrand 100 μl borosilicate glass, Scientific Laboratory Supplies, Germany) were pulled using a Flaming/Brown P-97 horizontal micropipette puller (Sutter Instruments, USA) and had a resistance between 3 and 5.5 MΩ. A giga-ohm seal was formed between the patch pipette and the cell membrane and the pipette capacitance transients were cancelled before achieving the whole cell configuration. All experiments were begun in voltage clamp mode with holding potential at -60 mV at the time of entering whole cell mode. After entering the whole-cell mode, series resistance was adjusted to be lower than 20 mega-ohm. Resting membrane potential was tested and only neurons with membrane potentials more negative than -50 mV were used for recording. Data were acquired and analysed with pClamp10 software (Axon Instruments, USA) and whole cell currents and voltages were filtered at 1 kHz and sampled at 10 kHz.

RNA-seq. MAH cells were trypsinized and collected as a cell pellet before lysis. RNA extraction was performed with the miRNeasy Mini Kit (Qiagen) according to the manufacturer's instructions. Two samples from MAH cells grown in growth medium and 2 samples from MAH cells grown in differentiation medium were sent to Oxford Gene Technology to complete the rest of the steps for RNA-sequencing. Sequencing libraries were prepared with the Illumina TruSeq RNA Sample Prep Kit v2. A total of 4 samples (two cold-sensitive MAH cells and two cold-insensitive MAH cells) were sequenced on 2 lanes on the Illumina HiSeq2000 platform using TruSeq v3 chemistry. All sequences were paired-end and sequencing was performed over 100 cycles. Read files (Fastq) were generated from the sequencing

platform via the manufacturer's proprietary software. Reads were processed through the Tuxedo suite. Reads were mapped to their location to the appropriate Illumina iGenomes build using Bowtie version 2.0.2. Splice junctions were identified using TopHat, version v2.0.9. Cufflinks version 2.1.1 was used to perform transcript assembly, abundance estimation and differential expression and regulation for the samples. Visualization of differential expression results were performed with CummeRbund. RNA-seq alignment metrics were generated with Picard.

In situ hybridization following calcium imaging. Coverslips were marked on the periphery with a diamond knife to assist localization of the imaged region and were then calcium-imaged as above to identify novel heat-sensitive neurons. Following calcium imaging, coverslips were rinsed with phosphate-buffered saline (PBS) then fixed in 4% paraformaldehyde (PFA) at 4 °C for 20 min. TRPM2 mRNA was detected with digoxigenin-labelled antisense probes against mouse *Trpm2* (NM_138301.2). We are very grateful to Y. Mori of Kyoto University for providing the mouse *Trpm2* gene cloned into the pCI-neo plasmid (Promega).

Probe synthesis. For the *Trpm2* antisense probe the plasmid was linearized with EcoRI and transcribed with T3 RNA polymerase and for the *Trpm2* sense probe, which was used as a negative control, the plasmid was linearized with SalI and transcribed with T7 RNA polymerase.

Hybridization. Fixed coverslips were rinsed in PBS with 0.1% Triton, and were then incubated in *in situ* hybridization solution without probe at 47 °C for 30 min as pre-hybridization step. After pre-hybridization, coverslips were transferred into *in situ* hybridization solution with antisense or sense probes for hybridization at 47 °C overnight²⁹.

Post-hybridization steps. Following hybridization coverslips were washed in 2 × SSC and then 0.2 × SSC at 47 °C for 30 min for each solution. Coverslips were then washed twice with KTBT solution at room temperature for 5 min for each washing. 25% normal goat serum was then used for blocking cells for 1 h at room temperature. Coverslips were then incubated in 25% normal goat serum containing pre-absorbed anti-digoxigenin antibody coupled to alkaline phosphatase for 2 h at room temperature, followed by washing 3 × in KTBT for 15 min each wash, and then twice in alkaline phosphatase buffer at room temperature for 10 min each wash. Coverslips were then developed in alkaline phosphatase buffer containing 337.5 μg ml⁻¹ NBT and 175 μg ml⁻¹ BCIP in the dark for 8 h before being washed in KTBT, fixed in 4% PFA for 10 min, washed in PBS, and then mounted in SlowFade Gold Antifade Mountant with DAPI²⁹. DIC transmitted-light images were acquired through a Plan Fluor 10 × Ph1 DLL objective with a DS-Qi2 monochrome camera on a Nikon Eclipse Ti-E inverted microscope. A GFPHQ filter was used to enhance the dark purple colour. The images were rotated, cropped, and resized with ImageJ to be aligned with the images obtained in calcium imaging.

Staining for isolectin B4 (IB4) following calcium imaging. DRG neurons on marked coverslips were calcium imaged as above then rinsed with phosphate-buffered saline (PBS) and fixed in 4% paraformaldehyde (PFA) at 4 °C for 20 min. After fixation, coverslips were washed twice in PBS with 0.1% Triton then incubated in solution containing 10 μg ml⁻¹ IB4 bound to Alexa Fluor 594, 10% normal goat serum, 2% bovine serum albumin, 0.1% Triton, and 10 mM sodium azide for 1 h at room temperature followed by washing with PBS three times. DIC transmitted-light images were acquired through a Plan Fluor 10 × Ph1 DLL objective with a DS-Qi2 monochrome camera on a Nikon Eclipse Ti-E inverted microscope. A Texas Red HYQ filter was used to capture the Alexa 594 signal. The images obtained were rotated, cropped, and resized with ImageJ to be aligned with the images obtained in calcium imaging.

Two-plate thermal preference tests. To eliminate as far as possible any extraneous genetic influences the *Trpm2*^{-/-} mice were backcrossed onto the parental

C57Bl6/6J line for 7 generations^{27,28}. To minimize environmental effects, wild-type and *Trpm2*^{-/-} littermates from heterozygous matings were compared in behavioural experiments. Sample size to achieve significance was determined from trial experiments but no power analysis was performed. All mice were tested at all temperatures so no randomization of experimental groups was necessary (see Fig. 3 legend). We used a two-plate thermal preference test (BioSeb, France) with one plate maintained at a temperature of 33 °C, which other studies have shown is the preferred temperature¹¹, and the other at a variable temperature. The temperatures of test and control plates were reversed after 30 min to control for any influence of environmental cues. Other studies have observed sex differences in mouse thermal behaviour¹² so we followed other authors^{5,11} in using only adult males (10–16 weeks old) in behavioural experiments.

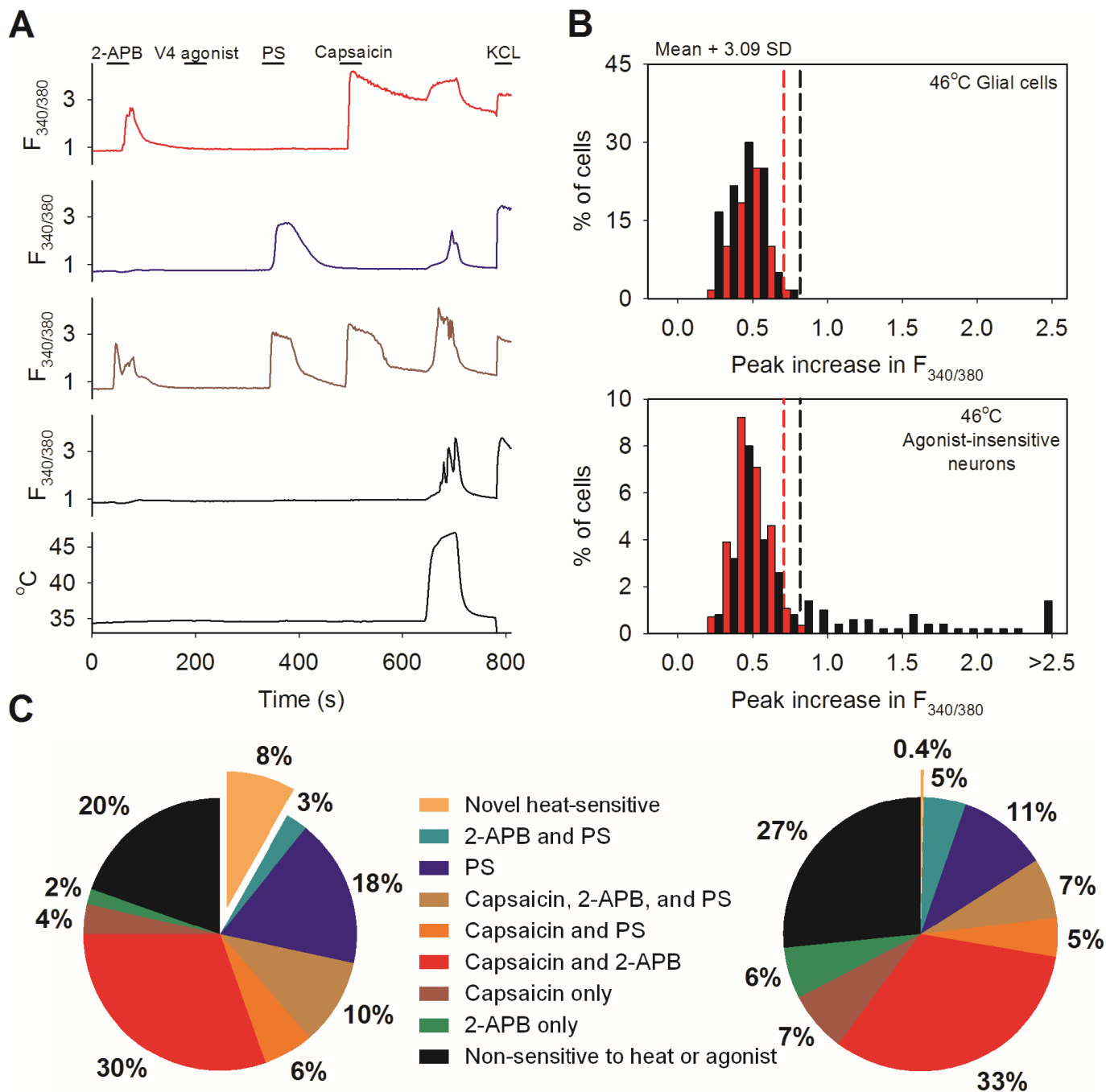
Two hot/cold-plate machines (Bioseb, France), placed back to back, formed the two-plate thermal apparatus. Plates were enclosed in a plexiglass chamber divided into two lanes, with an opaque compartment between them, and two mice were tested simultaneously in adjacent lanes (see Supplementary Information Video 2). The temperature of each plate was controlled by T2CT software (Bioseb, France). Plate temperatures were tested with an infrared thermometer (Bioseb) and were found to be accurately controlled to within 0.2 °C of the command temperature over the entire plate area. One plate was maintained at the preferred temperature of 33 °C, and mice were initially placed onto the plate with starting temperature other than 33 °C ('plate A', see Fig. 3) before initiating recording. The movements of the mice between the two plates were recorded for 3,495 s without human presence and the mouse position was determined with an automated video tracking system (Bioseb), so operator blinding was not necessary. The temperatures of the two plates were exchanged 1,800 s after initiation of recording; plate temperature settled to within 0.2 °C of the new temperature within 180 s of the change. Experiments were performed between 8 a.m. and 10 p.m., with room temperature at 20 °C. For experiments testing thermal preference between the two mildest temperatures, 28 °C versus 33 °C and 33 °C versus 38 °C, mice were tested again, with the starting temperatures of the two plates exchanged, 3–5 h after the first recording. For other temperatures recordings were made only once on a particular mouse. Mice were tested with the protocols, in order, of 28 °C versus 33 °C, 33 °C versus 38 °C, 23 °C versus 33 °C and 33 °C versus 43 °C. Sample size was based on pilot experiments. When making statistical comparisons variances were checked to ensure that it was similar between groups being compared. All animal experiments were approved by the Animal Welfare and Ethical Review Body (AWERB), King's College London.

Supplementary Information Video 2 shows an example of a thermal-choice behavioural experiment.

Statistical analysis. All data are expressed as means ± s.e.m. Analyses were performed with GraphPad Prism version 6.01 or SigmaPlot 11.0. The particular statistical test used is stated either in the text or figure legends.

Biological and technical replicates. Biological replicates are stated in the legends for each figure. Given the nature of these experiments, technical replicates were not possible.

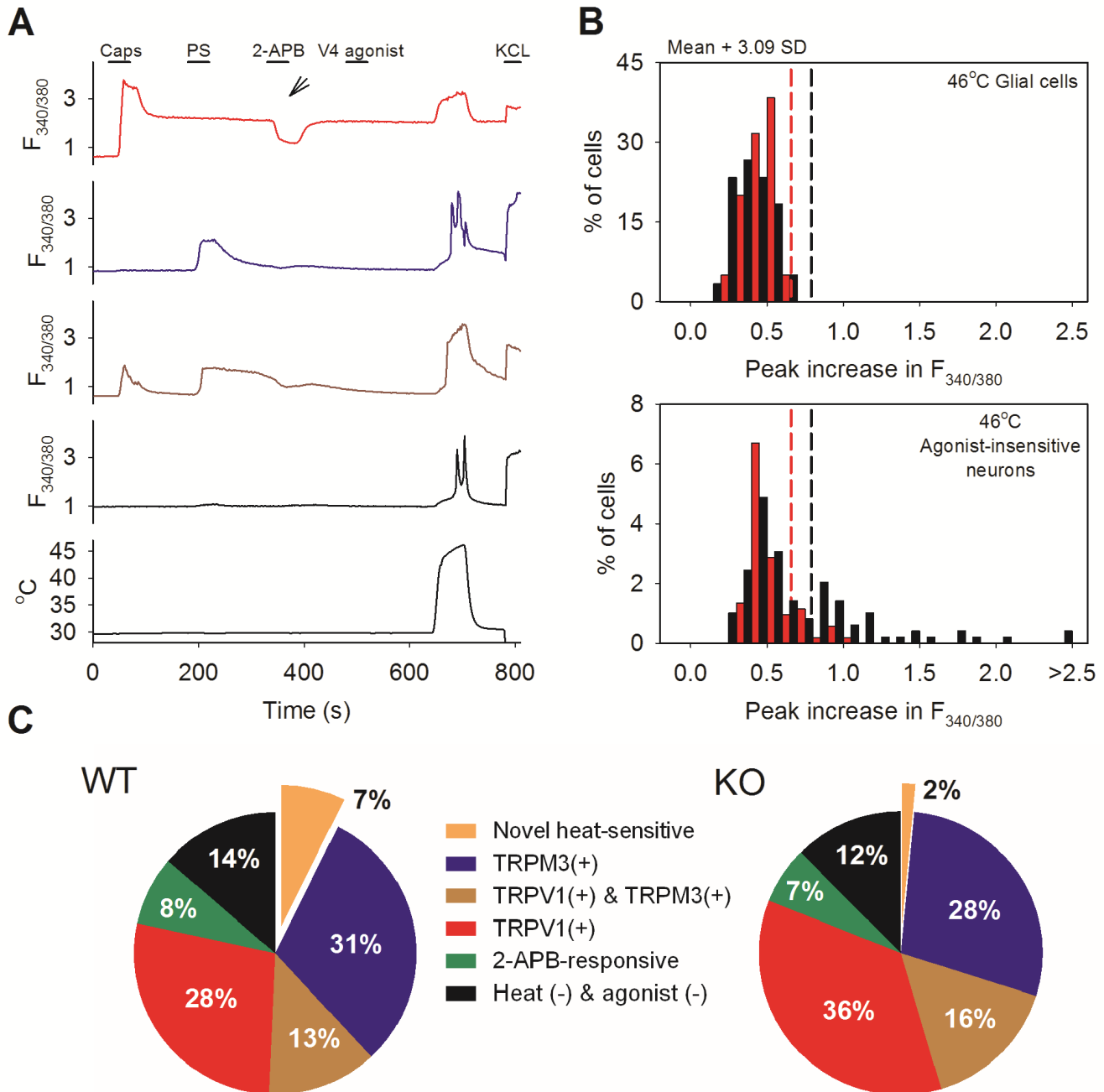
- Ariza-McNaughton, L. & Krumlauf, R. Non-radioactive *in situ* hybridization: simplified procedures for use in whole-mounts of mouse and chick embryos. *Int. Rev. Neurobiol.* **47**, 239–250 (2002).
- Schmid, D., Messlinger, K., Belmonte, C. & Fischer, M. J. Altered thermal sensitivity in neurons injured by infraorbital nerve lesion. *Neurosci. Lett.* **488**, 168–172 (2011).
- Jang, Y. *et al.* TRPM2 mediates the lysophosphatidic acid-induced neurite retraction in the developing brain. *Pflugers Arch.* **466**, 1987–1998 (2014).



Extended Data Figure 1 | See next page for caption.

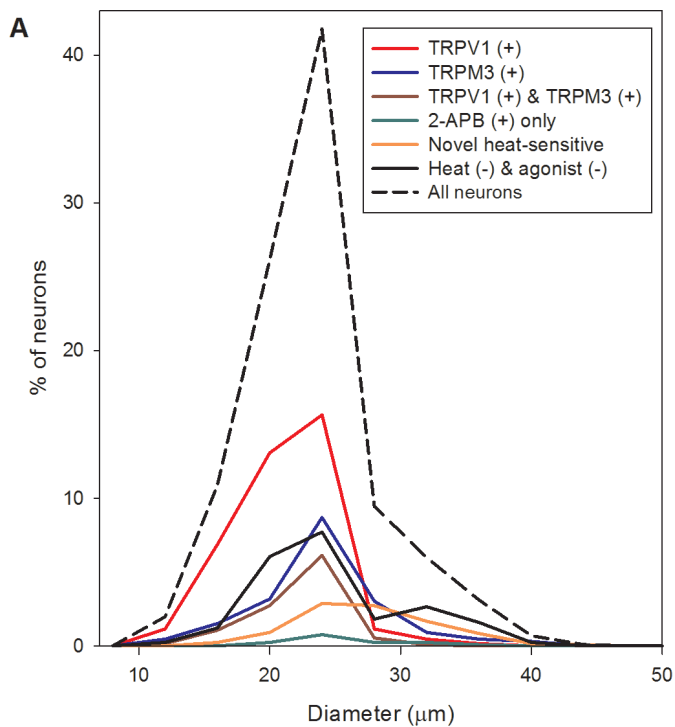
Extended Data Figure 1 | Effect of altering the order of agonist application in DRG neurons a, Method for detecting novel heat-sensitive somatosensory neurons. Representative traces showing increases of $[Ca^{2+}]_i$ ($F_{340/380}$ ratio, ordinate) in DRG neurons in response to the TRPV1-3 agonist 2-APB ($250 \mu\text{M}$), to the specific TRPV4 agonist PF-4674114 (V4 agonist, 200 nM), to the specific TRPV1 agonist capsaicin ($1 \mu\text{M}$), to the TRPM3 agonist pregnenolone sulphate (PS, $100 \mu\text{M}$), to a heat ramp from 35°C to 46°C (temperature protocol shown at bottom), and to KCl (50 mM). Other details as in Fig. 1. From top: TRPV1-expressing neuron responding to 2-APB, capsaicin ($1 \mu\text{M}$) and heat (red, 30% of 500 neurons); TRPM3-expressing neuron responding to PS (blue, $100 \mu\text{M}$) and heat (18%); TRPV1- and TRPM3-co-expressing neuron responding to 2-APB, PS, capsaicin, and heat (brown, 10%); neuron unresponsive to TRP channel agonists but showing a response to heat and therefore expressing a novel heat sensitive ion channel (black, 8% of total). No neuron responded to the specific TRPV4 agonist PF-4674114 (200 nM). **b**, Heat has a small effect on the fura-2 fluorescence ratio³⁰, so we eliminated neurons in which an increase of fluorescence ratio was due simply to this physical effect by comparing the increase of fura-2 fluorescence ratio in neurons with that in glial cells in the same culture. Maximum increases in $F_{340/380}$ ratio in response to a heat ramp from 35°C to 46°C in wild-type glial cells (black bars, top, $n = 60$) and in

wild-type DRG neurons not responding to known thermo-TRP agonists (black bars, bottom, from same images as the glial cells in top panel, $n = 139$). Vertical black dashed line in top panel shows mean $+ 3.09$ s.d. (cumulative probability value of 99.9%) of the increase in the $F_{340/380}$ ratio in glial cells; this value is taken as the maximum increase in $F_{340/380}$ ratio caused by effect of heat on fura-2 and is used as the cut-off value for defining novel heat-sensitive neurons present in the same culture dish (vertical black dashed line in lower panel). Similar results from separate culture of *Trpm2*^{-/-} glia ($n = 40$) and neurons ($n = 76$) shown in red. The proportion of novel heat-sensitive neurons was significantly reduced from 8% ($41/500$) in wild type to 0.4% ($1/282$) in *Trpm2*^{-/-} ($P \leq 0.0001$; Fisher's exact test). The increases in $F_{340/380}$ ratio of novel heat-sensitive neurons above the cut-off value in response to heat (smallest increase = 0.019854) are all higher than that of the single heat-responding *Trpm2*^{-/-} neuron (0.019084). **c**, Pie charts showing the percentage of novel heat-sensitive neurons responding to TRP ion channel agonists and to heat in wild-type DRG neurons (left) and DRG neurons from *Trpm2*^{-/-} mice (right). Deletion of *Trpm2* reduces the percentage of novel heat-sensitive neurons from 8% to 0.4%. Cell numbers for **a–c** were 500 DRG neurons from one wild-type mouse on 3 coverslips and 282 DRG neurons from one *Trpm2*^{-/-} mouse on 2 coverslips imaged. No further replicates of this particular experimental protocol were performed.



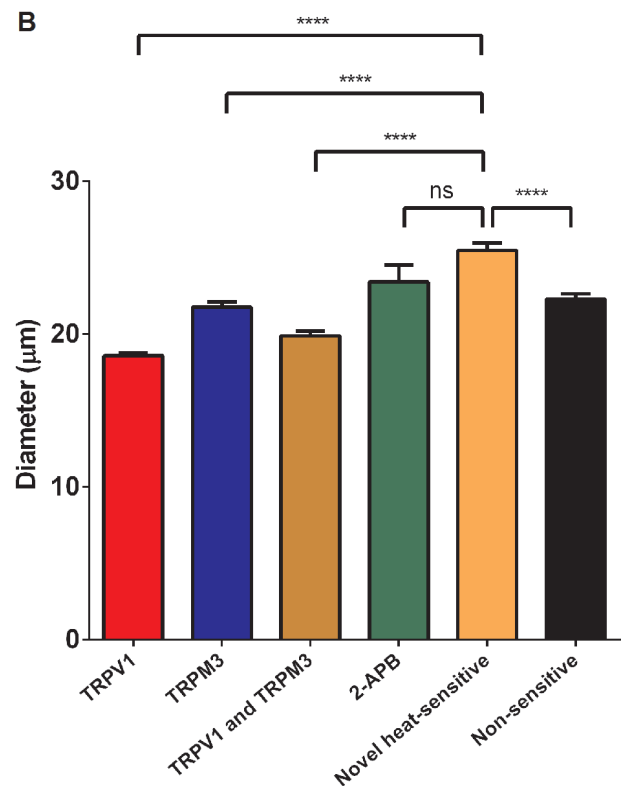
Extended Data Figure 2 | Effect of starting the heat ramp at a lower temperature in DRG neurons. Identical experiment to that shown in Fig. 1a–c, except that the temperature ramp started from 30°C. **a**, Agonist and heat-responsive neurons as in Fig. 1a. From top: TRPV1-expressing neuron responding to capsaicin (1 μM) and heat (red, 28% of 491 neurons); TRPM3-expressing neuron responding to PS (blue, 100 μM) and heat (31%); TRPV1- and TRPM3-co-expressing neuron responding to capsaicin, PS and heat (brown, 13%); neuron unresponsive to TRP channel agonists but showing a response to heat and therefore expressing a novel heat-sensitive ion channel (black, 7% of total). A small number of neurons (8%) responded to 2-APB (250 μM) but not to other agonists, and 14% of DRG neurons did not respond to any of the agonists nor to heat (not shown). No neuron responded to the specific TRPV4 agonist PF-4674114 (200 nM). **b**, Maximum increases in $F_{340/380}$ ratio in response to a heat ramp from 30°C to 46°C in wild-type glial cells (black bars, top, $n = 60$) and in heat-sensitive wild-type DRG neurons not responding to known thermo-TRP agonists (black bars, bottom, from same images as the glial cells in top panel, $n = 103$). Vertical black dashed line in top panel shows

mean + 3.09 s.d. (cumulative probability value of 99.9%) of the increase in the $F_{340/380}$ ratio in glial cells; this value is taken as the maximum increase in $F_{340/380}$ ratio caused by effect of heat on fura-2 and is used as the cut-off value for defining novel heat-sensitive neurons present in the same culture dish (vertical black dashed line in lower panel). Similar results from separate culture of *Trpm2*^{-/-} glia ($n = 60$) and neurons ($n = 73$) shown in red. The proportion of novel heat-sensitive neurons was significantly reduced from 7% (103/491) in wild type, to 2% (73/522) in *Trpm2*^{-/-} ($P \leq 0.0001$; Fisher's exact test). The mean increase in $F_{340/380}$ ratio of novel heat-sensitive neurons above the cut-off values in response to heat was also significantly reduced from 1.237 ± 0.09207 in wild type ($n = 36$) to 0.7959 ± 0.03767 in *Trpm2*^{-/-} ($n = 8$) ($P = 0.0313$; two-tailed unpaired *t*-test). **c**, Pie charts showing the percentage of novel heat-sensitive and TRPV1- or TRPM3-expressing neurons in wild-type DRG neurons (left) and DRG neurons from *Trpm2*^{-/-} mice (right). Cell numbers for imaging in a–c were 491 DRG neurons from one wild-type mouse on 3 coverslips and 522 DRG neurons from one *Trpm2*^{-/-} mouse on 3 coverslips. No further replicates of this particular experimental protocol were performed.

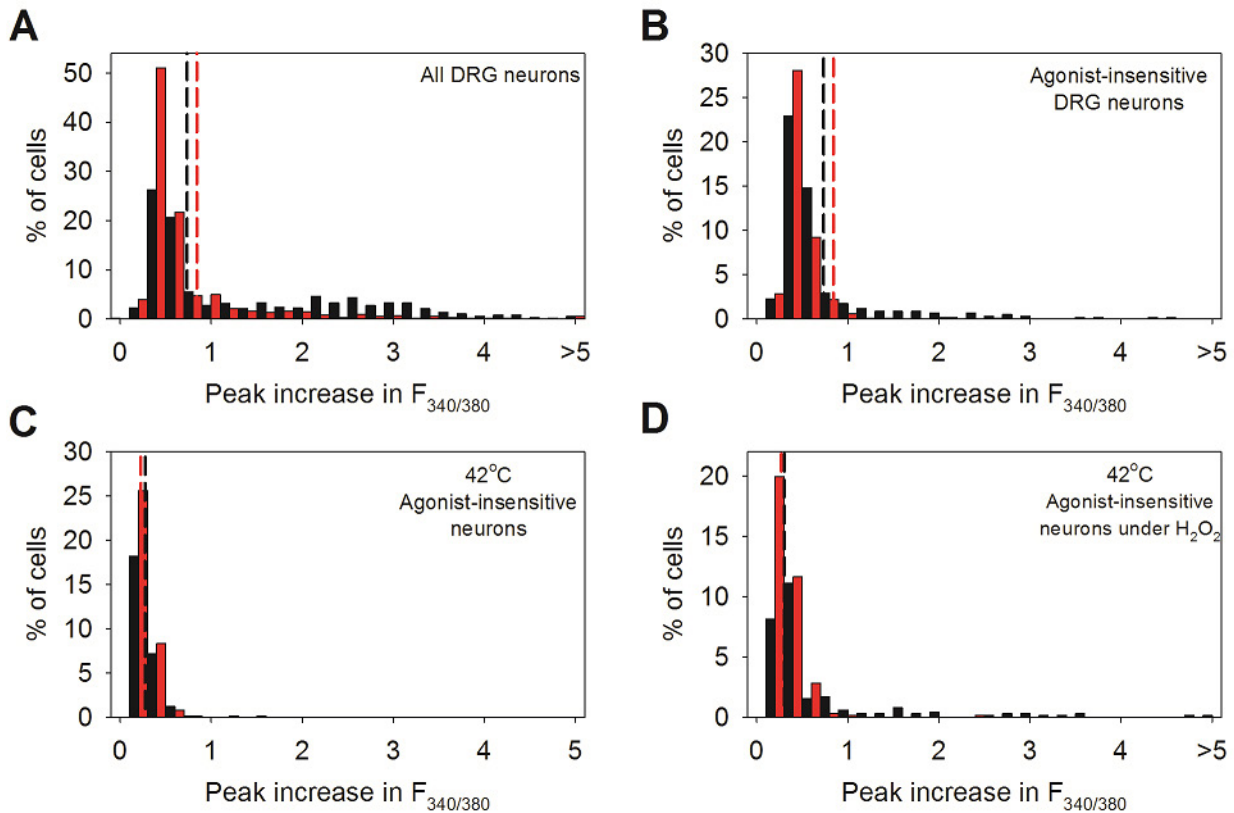


Extended Data Figure 3 | Diameters of novel heat-sensitive DRG neurons compared to neurons responding to other TRP agonists.

a, Diameters of 1,324 DRG neurons taken from experiment illustrated in Fig. 1a (dotted line). Subpopulations of neurons are shown as follows: those responding to capsaicin and thus expressing TRPV1 (red); to PS and thus expressing TRPM3 (blue); to both agonists and thus co-expressing TRPV1 and TRPM3 (brown); to 2-APB alone (green); novel heat-sensitive neurons (orange), and neurons responding neither to heat nor to any of these agonists (black). **b**, Diameter comparison of subpopulations of

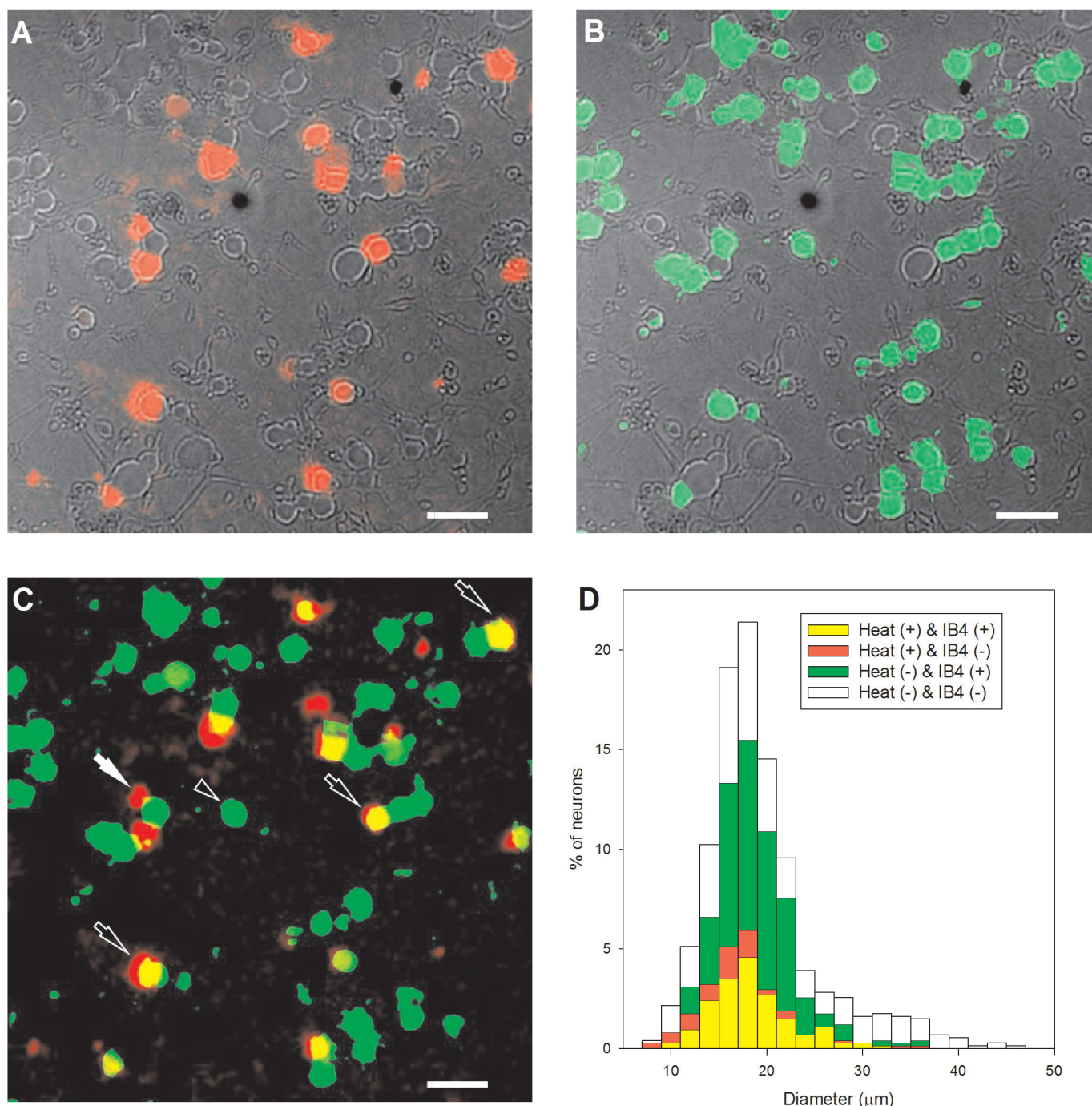


neurons. TRPV1-expressing neurons have the smallest mean diameter ($18.58 \pm 0.17 \mu\text{m}$), TRPM3-expressing neurons are intermediate ($21.75 \pm 0.33 \mu\text{m}$), and neurons expressing only the novel heat-sensitivity have the largest mean diameter ($25.47 \pm 0.48 \mu\text{m}$). Significance from one-way ANOVA and multiple comparisons with Tukey's multiple comparison test ($****P \leq 0.0001$; NS, not significant). Data obtained from Fig. 1a–c; 1,324 DRG neurons from one wild-type mouse on 4 coverslips were analysed.



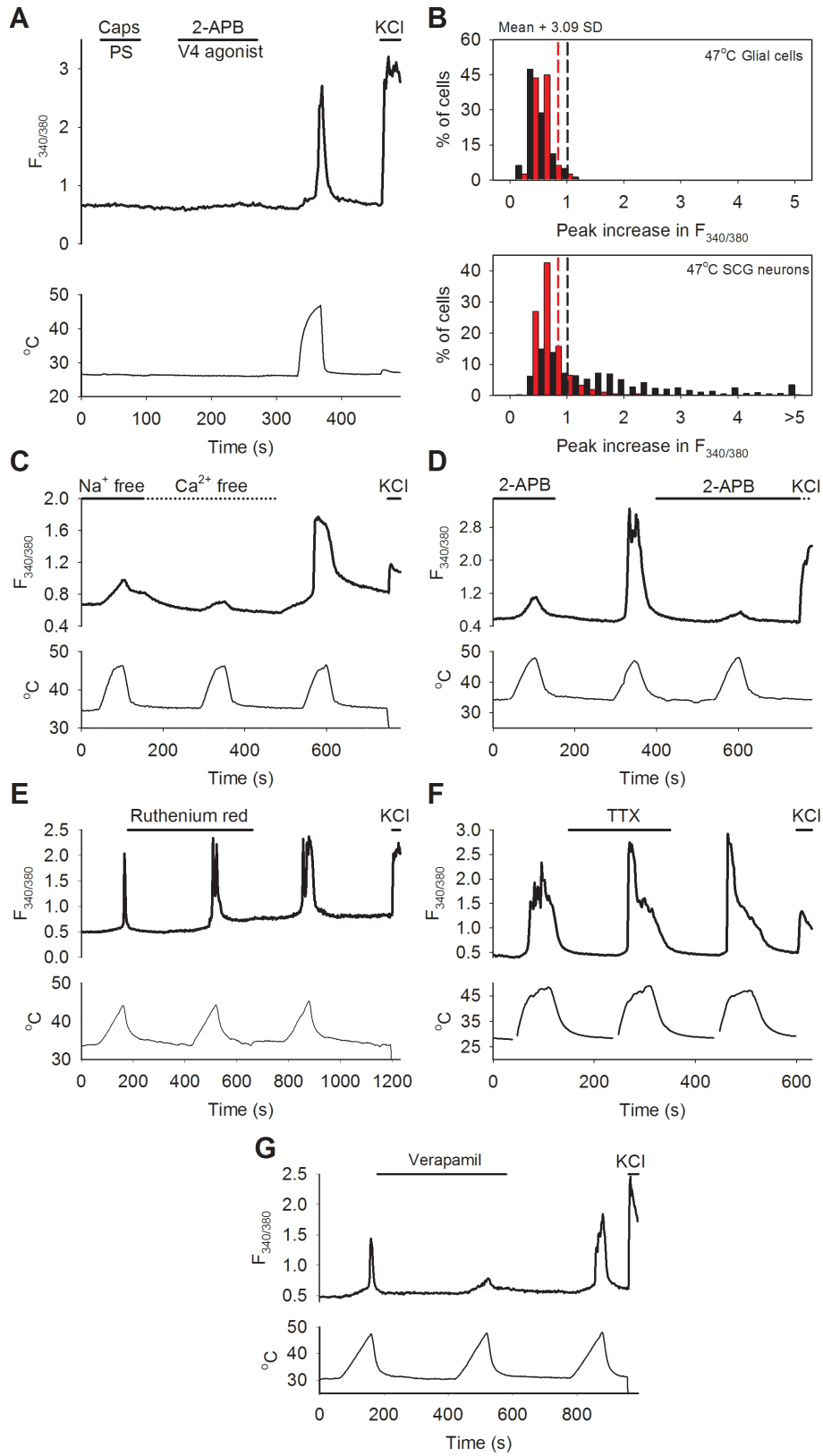
Extended Data Figure 4 | The novel heat-sensitivity in DRG neurons is partially co-expressed with TRPV1 and TRPM3, and is enhanced by H₂O₂. **a**, Temperature ramp to 47 °C, as in Fig. 1a, but with TRPV1 blocked with AMG9810 (5 μM) and TRPM3 blocked with naringenin (10 μM). Criterion level for significant increase (dashed lines) taken from glial cells in same field of view (data not shown). Black bars: 46% of all wild-type DRG neurons ($n = 580$) responded to heat ramp from 34 °C to 46 °C with an increase in [Ca²⁺]_i above criterion level in presence of blockers of TRPV1 and TRPM3 (dashed vertical line), while the percentage decreased to 17% in *Trpm2*^{-/-} DRG neurons (red bars, $n = 1,007$) ($P \leq 0.0001$; Fisher's exact test). The mean increase in F_{340/380} ratio above the cut-off values (dashed lines) in response to heat was also significantly reduced from 1.619 ± 0.06133 in wild type ($n = 265$) to 1.027 ± 0.08394 in *Trpm2*^{-/-} ($n = 175$) ($P \leq 0.0001$; two-tailed unpaired *t*-test). In similar experiments with TRPV1 blocker BCTC (4 μM) and naringenin (10 μM), 37% of wild-type neurons responded to heat (data not shown, $n = 554$). **b**, Similar plot as in **a**, but data from the subgroup of novel heat-sensitive neurons not responding to agonists for known thermo-TRP channels. After exposure to heat in presence of blockers of TRPV1 and TRPM3, blockers were removed and neurons not responding to known TRP agonists were identified as in Fig. 1a. Data from same experiment as shown in **a**. Proportion of neurons expressing the novel heat-sensitive mechanism in isolation (that is, without co-expression of TRPV1 or TRPM3) was significantly lower (52/580, 9%) than all neurons expressing the novel heat-sensitive mechanism (46%, see **a**).

The proportion of novel heat-sensitive neurons was significantly reduced in *Trpm2*^{-/-} mice, from 9% to 0.6% (6/1,007, $P \leq 0.0001$; Fisher's exact test). **c**, Temperature ramp to 42 °C. Few novel heat-sensitive neurons respond to this low temperature in either wild type or *Trpm2*^{-/-}. The total number of neurons was $n = 173$ for wild type and $n = 211$ for *Trpm2*^{-/-}. **d**, Responses of the same neurons to the same temperature ramp to 42 °C following addition of H₂O₂ (400 μM). Enhancement of response in wild type (black bars) was largely abolished in *Trpm2*^{-/-} (red bars). The proportion of novel heat-sensitive neurons after sensitization with H₂O₂ was significantly reduced from 11% (74/635) in wild type to 8% (48/601) in *Trpm2*^{-/-} ($P = 0.0356$; Fisher's exact test). The mean increase in F_{340/380} ratio of novel heat-sensitive neurons above the cut-off values in response to heat was also significantly reduced from 1.175 ± 0.1516 in wild type ($n = 72$) to 0.4485 ± 0.04329 in *Trpm2*^{-/-} ($n = 48$) ($P = 0.0002$; two-tailed unpaired *t*-test). Cell numbers and replicates for **a** and **b** were 580 DRG neurons from one wild-type mouse on 5 coverslips and 1,007 DRG neurons from one *Trpm2*^{-/-} mouse on 5 coverslips imaged for the protocol with AMG9810. 554 neurons from one wild-type mouse on 4 coverslips were imaged for the protocol with BCTC. No further replicates were carried out. The cell numbers and replicates for **c** and **d** were 635 DRG neurons from one wild-type mouse on 3 coverslips and 601 DRG neurons from one knockout mouse on 3 coverslips imaged. The experiment was replicated with similar results on 4 additional coverslips from one mouse.



Extended Data Figure 5 | Most novel heat-sensitive DRG neurons are IB4-positive. **a**, Increases in $[Ca^{2+}]_i$ ($F_{340/380}$ ratio image, intensity-coded in red, in mouse DRG neurons) in response to heat ramp to 46°C (TRPV1 blocked with AMG9810, 5 μ M, and TRPM3 blocked with naringenin, 10 μ M), superimposed on differential interference contrast (DIC) transmission image obtained post-fixation. **b**, The same field following fixation and labelling with fluorescent IB4 (green). **c**, Superimposed calcium and IB4 images from **a** and **b**. Black arrows show neurons responding to heat and positive for IB4. White arrow indicates a neuron responding to heat and negative for IB4. Black arrowhead shows neuron insensitive to heat and positive for IB4. Scale bars 50 μ m. **d**, Diameter histogram of 743 fixed DRG

neurons subgrouped according to novel heat-sensitivity (yellow, red) and IB4 binding (yellow, green). 25% (184/743) of DRG neurons showed novel heat-sensitivity, and 74% of these novel heat-sensitive neurons were IB4-positive, whereas only 53% of heat-insensitive neurons were IB4-positive. The percentage of IB4-positive neurons is significantly higher in the heat-sensitive group than in the heat-insensitive group ($P \leq 0.0001$; Fisher's exact test). The diameters shown in **d** are not directly comparable with the live cell diameters shown in Extended Data Fig. 3 because of a shrinkage artefact on fixation. Cell numbers were 743 DRG neurons from one wild-type mouse on 4 coverslips imaged. No further replicates were performed.

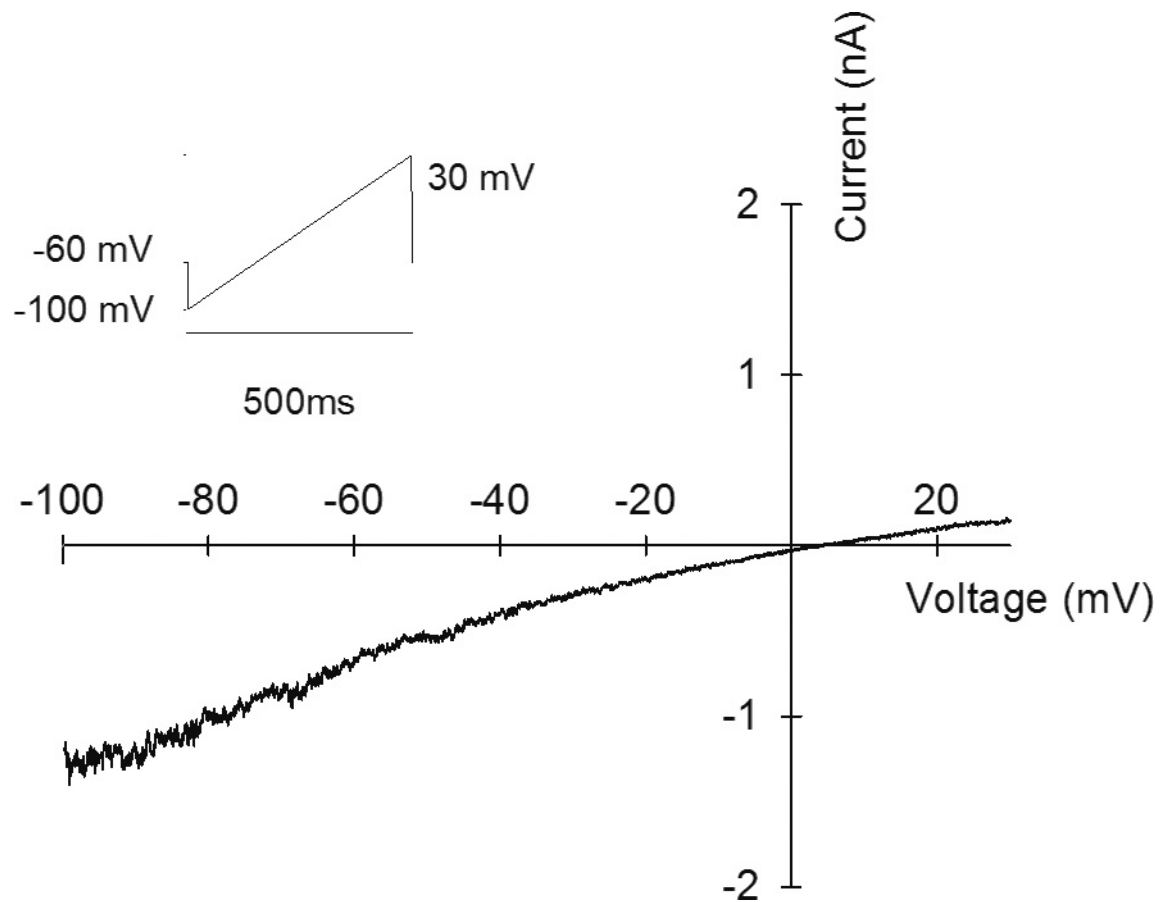


Extended Data Figure 6 | See next page for caption.

Extended Data Figure 6 | Properties of novel heat-sensitive ion channel expressed in autonomic neurons.

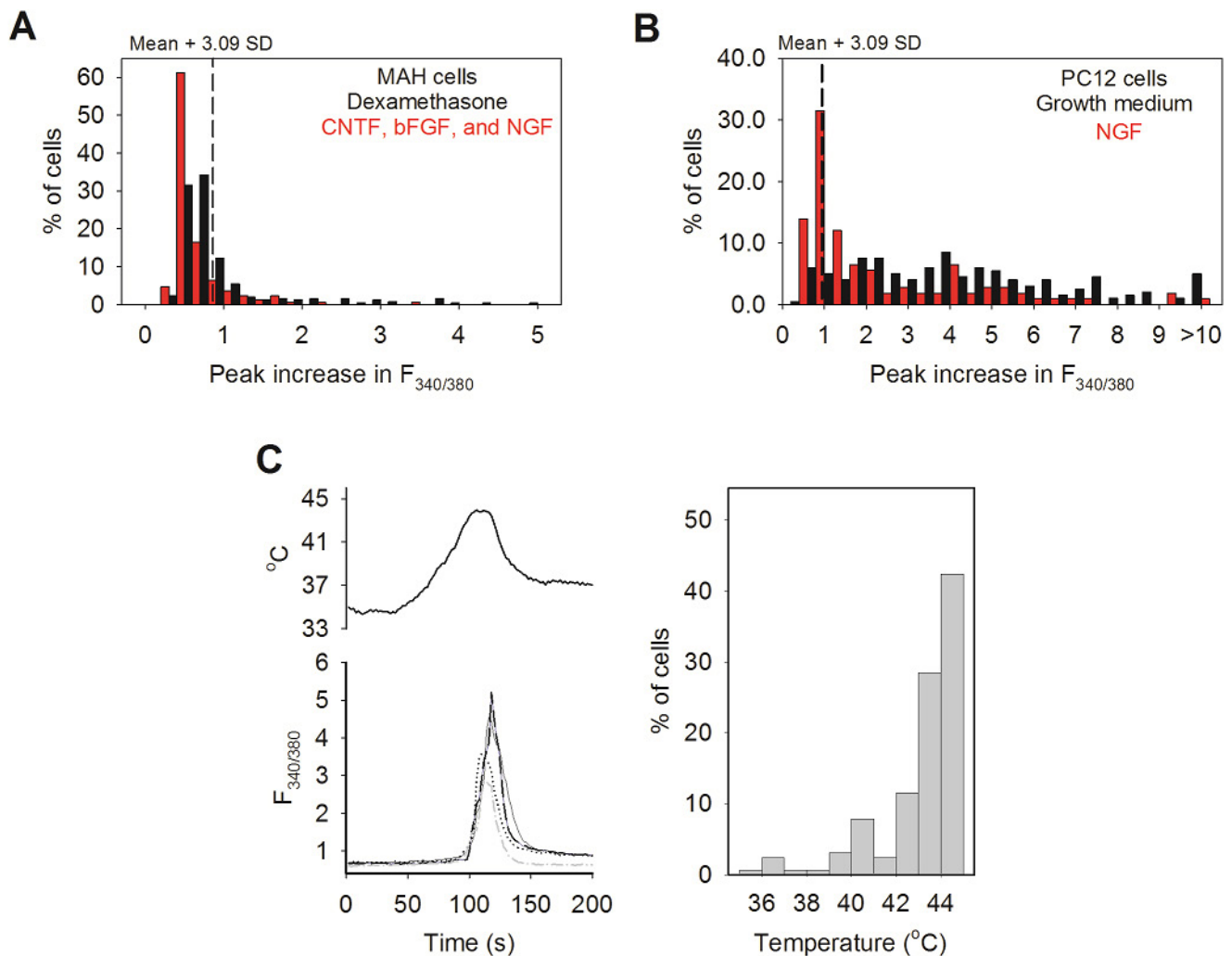
a, Representative traces showing increases of $[Ca^{2+}]_i$ ($F_{340/380}$ ratio, ordinate) in sympathetic neurons from superior cervical ganglion (SCG) in response to a mixture of capsaicin (TRPV1 agonist, 1 μ M) and pregnenolone sulphate (TRPM3 agonist, 100 μ M); a mixture of 2-APB (TRPV1-3 agonist, 250 μ M) and PF-4674114 (TRPV4 agonist, 200 nM); heat to 47 °C (temperature protocol shown at bottom); and KCl (50 mM). Similar results were obtained with parasympathetic neurons from pterygopalatine ganglion (PPG, data not shown). Trace is same as shown in Fig. 2a. **b**, Similar histograms as in Extended Data Figs 1b and 2b, but for SCG glial cells and neurons from wild-type mice (black bars) and *Trpm2*^{-/-} mice (red bars). 58% of wild-type SCG neurons ($n = 436$) showed novel heat-sensitivity with increases in $F_{340/380}$ ratio above the criterion level obtained from glial cells ($n = 80$) in same culture (black vertical dashed line). In similar experiments on PPG neurons ($n = 484$), 47% showed novel heat-sensitivity (not shown). Red bars and red dashed line show results from SCG glia ($n = 80$) and neurons ($n = 430$) from *Trpm2*^{-/-} mice. The proportion of novel heat-sensitive neurons was significantly reduced by deletion of *Trpm2*, from 58% (252/436) in wild type to 12% (53/430) in *Trpm2*^{-/-} ($P \leq 0.0001$; Fisher's exact test). The mean increase in $F_{340/380}$ ratio of heat-sensitive neurons above the cut-off values in response to heat was also significantly reduced, from 1.629 ± 0.1928 in wild type ($n = 252$) to 0.5050 ± 0.1270 in *Trpm2*^{-/-} ($n = 53$) ($P = 0.0086$; two-tailed unpaired *t*-test). **c**, Heat-evoked Ca^{2+} increase in SCG neurons is reduced but not abolished by removal of extracellular Na^+ (replaced with choline) and is abolished by removal of extracellular Ca^{2+} (remaining small increase in $F_{340/380}$ ratio

is due to temperature sensitivity of fura-2, see **b**). Similar results were seen in 133 SCG neurons. **d**, Heat-evoked Ca^{2+} increase in SCG neurons is blocked by TRPV agonist 2-APB (25 μ M). Similar results were seen in 130 SCG neurons. **e**, The Ca^{2+} increase in PPG neurons is not affected by TRPV channel blocker ruthenium red (50 μ M). Similar results were seen in 75 PPG neurons. **f**, The Ca^{2+} increase in PPG neurons is not affected by the Na channel blocker tetrodotoxin (2 μ M). Similar results were seen in 35 PPG neurons. **g**, The Ca^{2+} influx in PPG neurons is reduced but not eliminated by the L-type Ca^{2+} channel blocker verapamil (100 μ M). Similar results were seen in 30 PPG neurons. Cell numbers and replicates for **a** were 166 SCG neurons from three wild-type mice on 3 coverslips imaged. Cell numbers and replicates for **b** were 436 SCG neurons from two wild-type mice on 4 coverslips and 430 SCG neurons from two *Trpm2*^{-/-} mice on 4 coverslips imaged. Similar results as those shown for wild-type obtained with 15 further coverslips of SCG neurons from 9 wild-type mice and 7 coverslips of PPG neurons from 6 wild-type mice. Cell numbers and replicates for **c** were 133 SCG neurons from 3 wild-type mice on 5 coverslips that showed similar responses. Cell numbers and replicates for **d** were 130 SCG neurons from 3 wild-type mice on 2 coverslips that showed similar responses. Similar results were also obtained for DRG neurons (4 coverslips from 1 mouse). Cell numbers and replicates for **e** were 75 PPG neurons from 3 wild-type mice on 4 coverslips that showed similar responses. Cell numbers and replicates for **f** were 35 PPG neurons from 3 wild-type mice on 4 coverslips that showed similar responses. Cell numbers and replicates for **g** were 30 PPG neurons from 3 wild-type mice on 2 coverslips that showed similar responses.



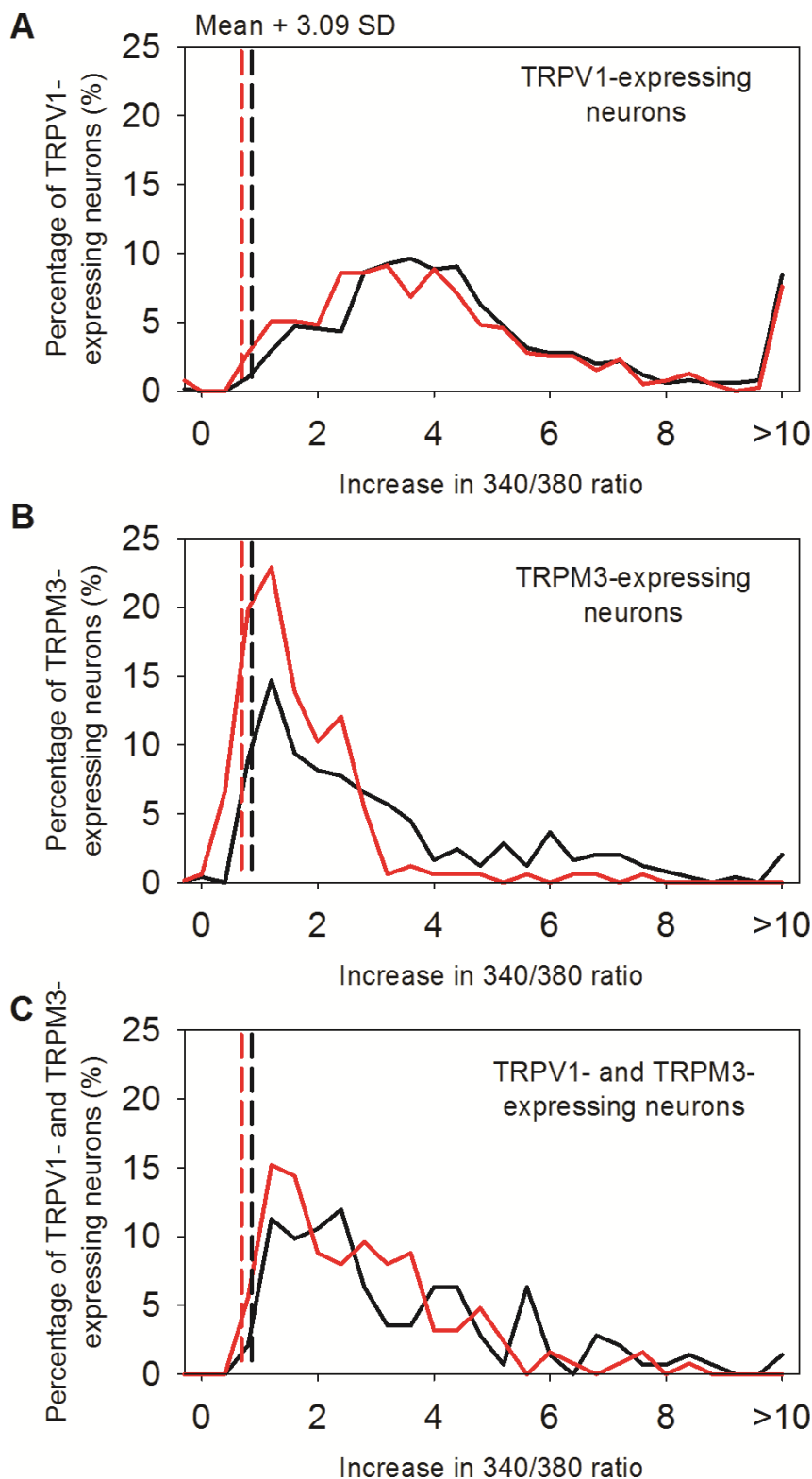
Extended Data Figure 7 | The heat-induced membrane current in autonomic neurons is not gated by membrane voltage. Current–voltage difference relations of a PPG neuron with a voltage ramp starting from a negative potential (inset) show a similar linear heat-induced current to

that obtained with reverse voltage ramp (see Fig. 2c). Trace obtained by subtracting current–voltage relations at 36 °C from that at 47 °C. Similar results were obtained in 3 cells on 3 coverslips.



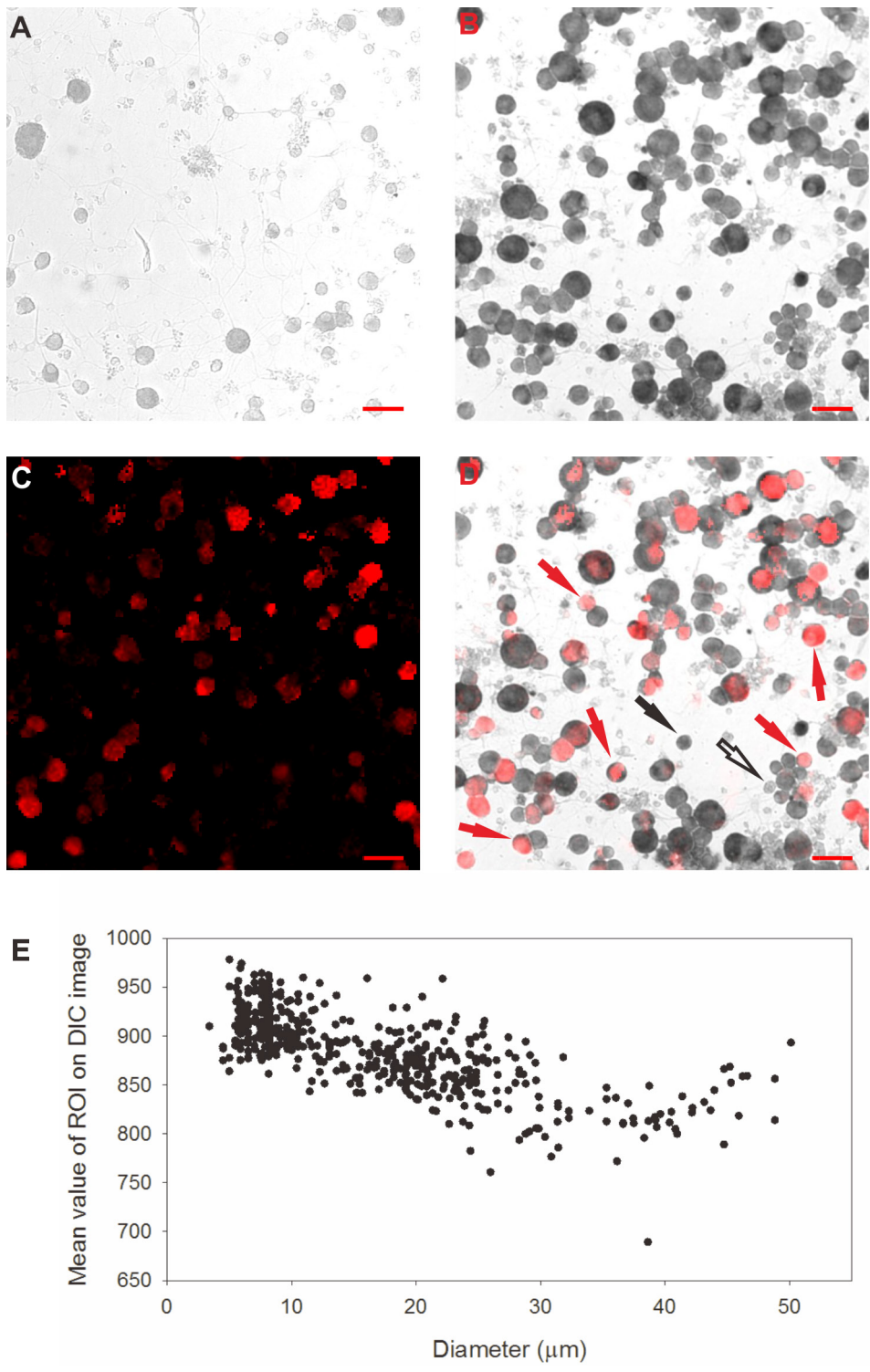
Extended Data Figure 8 | Responses to heat in adrenal-derived MAH and PC12 cell lines, and effects of factors causing differentiation to neuronal phenotype. **a**, MAH cells. Black indicates maximum increase in $F_{340/380}$ ratio in response to heat (47°C , $n = 254$) when cultured in dexamethasone ($5\ \mu\text{M}$). No cell responded to TRP agonists, but 27% of cells responded to heat with increase above mean criterion level obtained from glial cells in neuronal cultures (see Fig. 1b). Red indicates similar histogram after 12 days of culture in growth factors (bFGF, CNTF and NGF, see Methods, $n = 170$). No cell responded to TRP agonists; 9% responded to heat. The proportion of heat-sensitive cells was significantly reduced from 27% (69/254) in dexamethasone to 9% (16/170) in growth factors ($P \leq 0.0001$; Fisher's exact test). The 66% reduction in the proportion of heat-sensitive cells was not significantly different from the reduction in *Trpm2* expression caused by differentiation of MAH cells (Table 1; $P = 0.056$; two-tailed unpaired *t*-test). The mean increases in $F_{340/380}$ ratio above the cut-off values (dashed lines) in response to heat were 1.755 ± 0.1255 in dexamethasone ($n = 69$) and 1.420 ± 0.1474 in presence of growth factors ($n = 16$) ($P = 0.2203$; two-tailed unpaired *t*-test). **b**, PC12 cells. Black indicates culture in growth medium

(10% horse serum plus 5% fetal bovine serum, $n = 200$). 93% of cells responded to heat with increase above mean criterion level obtained from glial cells in neuronal cultures (see Fig. 1b). Red indicates effect on heat responses of 12 days of culture in NGF (1% horse serum plus $100\ \text{ng ml}^{-1}$ NGF, $n = 108$). The proportion of heat-sensitive cells was significantly reduced from 93% (186/200) in growth medium to 46% (50/108) in NGF ($P \leq 0.0001$; Fisher's exact test). We note that a significantly lower expression of mRNA for TRPM2 in differentiated PC12 cells has been reported³¹. The mean increase in $F_{340/380}$ ratio above the cut-off values (dashed lines) in response to heat was significantly reduced from 3.753 ± 0.2431 in growth medium ($n = 186$) to 2.603 ± 0.3104 in NGF ($n = 50$) ($P = 0.0213$; two-tailed unpaired *t*-test). **c**, Temperature thresholds of PC12 cells cultured in growth medium. Top left, temperature protocol. Bottom left, temperature responses of three representative cells. Right, temperature thresholds calculated as in Fig. 1d. Cell numbers and replicates for **a** and **b** were 2 coverslips for each condition imaged. Cell numbers are given above. Replicates of 4 coverslips (MAH cells) and 3 coverslips (PC12 cells) for each condition gave similar results. Cell numbers and replicates for **c** were 165 PC12 cells on one coverslip imaged.



Extended Data Figure 9 | Effect of deletion of TRPM2 on maximal calcium responses to heat in neurons expressing TRPV1 or TRPM3.
a, Maximum increases in $F_{340/380}$ ratio in response to a heat ramp from 34 °C to 46 °C in neurons responding only to capsaicin (TRPV1-expressing) from wild-type (black) and $Trpm2^{-/-}$ (red) mice. The increase in $F_{340/380}$ ratio in response to heat (above the increase caused by the effect of temperature on fura-2, vertical dotted lines, for method of calculation see Fig. 1b) is not significantly different between wild type and $Trpm2^{-/-}$ ($P=0.1168$, two-tailed Mann-Whitney U -test). Details as in Fig. 1. **b**, Neurons responding only to pregnenolone sulphate (PS, TRPM3-expressing) from the same experiments as in **a**. The increases

in $F_{340/380}$ ratio in response to heat are significantly reduced by deletion of $Trpm2$ (from 6.389 ± 1.225 to 4.411 ± 1.582 , $P < 0.0001$, two-tailed Mann-Whitney U -test). **c**, Neurons responding to both capsaicin and PS (TRPV1- and TRPM3-expressing). The increases in $F_{340/380}$ ratio in response to heat are not significantly different between wild type and $Trpm2^{-/-}$ ($P=0.0633$; two-tailed Mann-Whitney U -test). Cell numbers and replicates for **a-c** were 1324 DRG neurons from one wild-type mouse on 4 coverslips and 981 DRG from one $Trpm2^{-/-}$ mouse on 4 coverslips imaged. Similar results obtained from 42 additional coverslips from 6 wild-type mice and 8 additional coverslips from one $Trpm2^{-/-}$ mouse.



Extended Data Figure 10 | See next page for caption.

Extended Data Figure 10 | Correlation between novel heat sensitivity and expression of mRNA for TRPM2. **a**, Representative DIC transmission image of DRG neurons following *in situ* hybridization with the sense probe as negative control. Non-specific density was linearly dependent on cell diameter (see **e**). Mean + 3.09 s.d. (cumulative probability value of 99.9%) of density as a function of diameter with sense probe (5 μm bins) was used as threshold criterion for significant expression of *Trpm2* in images of antisense hybridization. A similar analysis of non-specific density was carried out for glial cells. **b**, Representative DIC transmission image with antisense probe against *Trpm2*. Using the threshold criterion as function of diameter obtained from sense probe images (see **a**), 89% (1,121/1,250) of DRG neurons but 3% (4/120) of glial cells were positive for TRPM2 mRNA. **c**, Novel heat-sensitive DRG neurons determined using calcium imaging. Increases in $[\text{Ca}^{2+}]_i$ ($F_{340/380}$ ratio image, intensity-coded in red) in response to a heat ramp to 46 °C with TRPV1 blocked with AMG9810 (5 μM) and TRPM3 blocked with naringenin (10 μM). **d**, Superimposed image of novel heat-sensitive neurons (red) and *in situ* hybridization using antisense probe. Solid red arrows indicate novel heat-sensitive neurons also positive for TRPM2; solid black arrow shows neuron not responding

to heat but positive for TRPM2; open black arrow shows cell negative for TRPM2 (that is, with density below the criterion level obtained from **e**). 42% (92/218) of DRG neurons positive for TRPM2 exhibited novel heat-sensitivity. However only 13% (2/16) of DRG neurons negative for TRPM2 from *in situ* hybridization exhibited novel heat-sensitivity. The percentage of novel heat-sensitive DRG neurons is significantly reduced in TRPM2 negative DRG neurons ($P = 0.0188$; Fisher's exact test). Scale bars, 50 μm . **e**, Density of non-specific label in neurons obtained from hybridization with sense probe (see **a**) depends on cell size. Data used to calculate significance thresholds for neurons in **b**. Cell numbers and replicates for **a** was one coverslip exposed to sense probe used as negative control. Cell numbers and replicates for **b** were all neurons on 5 coverslips measured and one coverslip was measured for TRPM2-positive glial cells. Cell numbers and replicates for **c** and **d** was one coverslip was analysed as in **a** and **b** for the combined calcium imaging and *in situ* hybridization protocol. Cell numbers and replicates for **e** were 500 DRG neurons on one coverslip exposed to the sense probe used to determine the background threshold as a function of cell diameter. Similar *in situ* hybridization results were obtained on 16 additional coverslips.